April 22, 2008

Sources of particulate matter in the northeastern United States in summer: 1. Direct emissions and secondary formation of organic matter in urban plumes

J. A. de Gouw
C. A. Brock
E. L. Atlas
T. S. Bates
F. C. Fehsenfeld, et al.

Sources of particulate matter in the northeastern United States in summer:

1. Direct emissions and secondary formation of organic matter in urban plumes

J. A. de Gouw,[1,2] C. A. Brock,[1] E. L. Atlas,[3] T. S. Bates,[4] F. C. Fehsenfeld,[1,2]
P. D. Goldan,[1,2] J. S. Holloway,[1,2] W. C. Kuster,[1] B. M. Lerner,[1,2] B. M. Matthew,[1,2,5]
A. M. Middlebrook,[1] T. B. Onasch,[6] R. E. Peltier,[7,8] P. K. Quinn,[4] C. J. Senff,[1,2] A. Stohl,[9]
A. P. Sullivan,[7,10] M. Trainer,[1] C. Warneke,[1,2] R. J. Weber,[7] and E. J. Williams[1,2]

[1] Ship and aircraft measurements of aerosol organic matter (OM) and water-soluble organic carbon (WSOC) were made in fresh and aged pollution plumes from major urban areas in the northeastern United States in the framework of the 2004 International Consortium for Atmospheric Research on Transport and Transformation (ICARTT) study. A large part of the variability in the data was quantitatively described by a simple parameterization from a previous study that uses measured mixing ratios of CO and either the transport age or the photochemical age of the sampled air masses. The results suggest that OM was mostly due to secondary formation from anthropogenic volatile organic compound (VOC) precursors in urban plumes. Approximately 37% of the secondary formation can be accounted for by the removal of aromatic precursors using newly published particulate mass yields for low-NOx conditions, which are significantly higher than previous results. Of the secondary formation, 63% remains unexplained and is possibly due to semivolatile precursors that are not measurable by standard gas chromatographic methods. The observed secondary OM in urban plumes may account for 35% of the total source of OM in the United States and 8.5% of the global OM source. OM is an important factor in climate and air quality issues, but its sources and formation mechanisms remain poorly quantified.

Citation: de Gouw, J. A., et al. (2008), Sources of particulate matter in the northeastern United States in summer: 1. Direct emissions and secondary formation of organic matter in urban plumes, *J. Geophys. Res.*, *113*, D08301, doi:10.1029/2007JD009243.

1. Introduction

[2] Particulate matter (PM) in the atmosphere is a pollutant that influences the Earth's climate directly through the scattering and absorption of solar radiation, and indirectly by providing the condensation nuclei for cloud droplets [*Ramanathan et al.*, 2001]. Organic matter (OM) (Table 1 gives a description of the acronyms used in this study for organic aerosol, and the measurement techniques to quantify them) accounts for a large and in many cases dominant fraction of the particulate mass [*Murphy et al.*, 2006; *Quinn and Bates*, 2003]. OM has both primary and secondary sources: direct emissions, and formation in the atmosphere through the (multistep) oxidation and subsequent condensation of gas-phase precursors, respectively [*Kanakidou et al.*, 2005]. However, the relative importance of the sources of OM and of its precursors is highly uncertain. It is the purpose of this study to investigate the sources of OM in urban plumes in the northeastern United States using measurements of OM, organic carbon (OC), water-soluble organic carbon (WSOC) and their gas-phase precursors. In a companion paper, the results are compared with the sources and formation of the inorganic PM component [*Brock et al.*, 2008].

[3] Numerous studies have attempted to quantify the primary and secondary, and the biogenic and anthropogenic

---

[1]Chemical Sciences Division, Earth System Research Laboratory, NOAA, Boulder, Colorado, USA.

[2]Also at Cooperative Institute for Research in Environmental Sciences, University of Colorado, Boulder, Colorado, USA.

[3]Rosenstiel School of Marine and Atmospheric Science, University of Miami, Miami, Florida, USA.

[4]Pacific Marine Environment Laboratory, NOAA, Seattle, Washington, USA.

[5]Now at Eastman Kodak Company, Windsor, Colorado, USA.

[6]Aerodyne Research Inc., Billerica, Massachusetts, USA.

[7]School of Earth and Atmospheric Sciences, Georgia Institute of Technology, Atlanta, Georgia, USA.

[8]Now at Department of Environmental Medicine, New York University School of Medicine, Tuxedo, New York, USA.

[9]Norwegian Institute for Air Research, Kjeller, Norway.

[10]Now at Department of Atmospheric Science, Colorado State University, Fort Collins, Colorado, USA.

Table 1. Summary of Acronyms Used in This Work

Acronym	Description	Measurement Used in This Study	Units
OM	organic matter (mass of particulate organic species)	AMS (aerosol mass spectrometry)	$\mu g\ m^{-3}$
OC	organic carbon (carbon mass of particulate organic species)	analysis of filter samples	$\mu g\ C\ m^{-3}$
WSOC	water-soluble organic carbon (carbon mass of water-soluble particulate organic species)	PILS-TOC (particle into liquid sampler–total organic carbon)	$\mu g\ C\ m^{-3}$

contributions to OM in the atmosphere, often with very different or even contradictory conclusions. Using measurements of tracer molecules, many studies have attributed a large fraction of OM to primary sources, including vehicle exhaust, food cooking and wood smoke, which together accounted for 85% of the OM at urban locations in California [*Schauer and Cass*, 2000; *Schauer et al.*, 1996]. Measurements of organic carbon (OC) and elemental carbon (EC), which is directly emitted from combustion sources, have been used to separate secondary from primary sources, since the OC/EC ratio increases as an air mass is photochemically processed. Such methods typically attribute the majority of OC in urban air to primary sources with occasional dominance of secondary sources [*Lim and Turpin*, 2002; *Turpin and Huntzicker*, 1995]. In contrast to these observations, recent studies using aerosol mass spectrometry (AMS) have indicated that a large fraction of OM in urban air is oxidized and not directly emitted from vehicles [*Lanz et al.*, 2006; *Zhang et al.*, 2005a, 2007]. To further confound the issue, radiocarbon dating indicates that a large fraction of the carbon in (sub-) urban OM is modern rather than fossil, suggesting that the sources are either secondary from gas-phase biogenic precursors, or primary from wood smoke [*Klinedinst and Currie*, 1999; *Lemire et al.*, 2002; *Szidat et al.*, 2004]. Studies in more remote regions have pointed at the importance of biogenic volatile organic compounds (VOCs) as OM precursors [*Claeys et al.*, 2004; *Tunved et al.*, 2006].

[4] The field studies above provide top-down estimates of the importance of different sources. Bottom-up estimates, based on emissions estimates and the results from smog chamber studies, indicate that primary emissions of OM from motor vehicles are relatively small [*Bond et al.*, 2004; *Kirchstetter et al.*, 1999], and that aromatic compounds in vehicle exhaust [*Ng et al.*, 2007b; *Odum et al.*, 1997] and terpenes from vegetation [*Hoffmann et al.*, 1997; *Kroll et al.*, 2005, 2006] are among the more efficient secondary OM precursors. As the global emissions of biogenic VOCs are much higher than those of anthropogenic, aromatic VOCs, most secondary formation of OM is expected from biogenic precursors [*Henze and Seinfeld*, 2006; *Kanakidou et al.*, 2005; *Tsigaridis and Kanakidou*, 2007]. On the other hand, atmospheric chemistry models that use the current best estimates of direct emissions and secondary formation generally do not reproduce the high levels of OM observed in polluted atmospheres [*Griffin et al.*, 2005; *Heald et al.*, 2005; *Johnson et al.*, 2006; *McKeen et al.*, 2007].

[5] In a previous paper, we have shown that the contribution of primary urban emissions of OM was relatively small in the northeastern United States, whereas positive correlations between OM and alkyl nitrates (gas-phase

oxidation products of anthropogenic emissions) suggested that a large fraction of OM was secondary and produced from anthropogenic precursors [*de Gouw et al.*, 2005]. Using the concept of photochemical age, we were able to show that a strong growth of OM occurs in urban plumes in the first 24 h after emission, and that this growth could not be explained using the commonly considered precursors. Since then, similar findings were reported for Mexico City [*Volkamer et al.*, 2006], London [*Johnson et al.*, 2006] and Tokyo [*Takegawa et al.*, 2006a]. The unexpectedly large growth in secondary OM was recently suggested to come from semivolatile organic compound (SVOC) precursors, which (1) partition from primary particles into the gas phase when vehicle emissions are diluted in ambient air, (2) become oxidized, and (3) condense onto existing particles thereby contributing to their growth [*Robinson et al.*, 2007].

[6] In our previous work, we developed a semiempirical parameterization that described the evolution of $\Delta OM/\Delta C_2H_2$ ratios in an air mass [*de Gouw et al.*, 2005]. (Here and elsewhere in the manuscript, Δ refers to an enhancement of a mixing ratio or concentration over the background value.) Here, we extend this equation to the case of $\Delta OM/\Delta CO$, $\Delta OC/\Delta CO$ and $\Delta WSOC/\Delta CO$ ratios. The equations derived are used for a quantitative comparison with the results of ship-based and airborne measurements of OM, OC and WSOC in the northeastern United States [*Peltier et al.*, 2007a; *Quinn et al.*, 2006; *Sullivan et al.*, 2006], which were conducted in the framework of the ICARTT (International Consortium for Atmospheric Research on Transport and Transformation) study in 2004 [*Fehsenfeld et al.*, 2006]. The airborne measurements, in particular, are of interest as it is more straightforward to identify urban plumes and their origin. Finally, detailed measurements of gas-phase volatile organic compounds (VOCs) are used to evaluate the secondary formation pathways of OM in urban plumes.

2. Measurements

[7] The data presented in this work were obtained on board the NOAA WP-3D research aircraft (WP-3D) and the NOAA research ship Ronald H. Brown (RHB) during the NEAQS-ITCT 2004 experiment (New England Air Quality Study–Intercontinental Transport and Chemical Transformation), which was the NOAA component of the ICARTT study (International Consortium for Atmospheric Research on Transport and Transformation) [*Fehsenfeld et al.*, 2006].

2.1. Field Measurements
2.1.1. Aircraft
[8] A total of 18 flights were made between 5 July and 15 August 2004, using the NOAA WP-3D aircraft based in

Portsmouth, New Hampshire, United States. Flight objectives included the characterization of emissions from cities in the eastern United States (e.g., New York City and Boston), power plants (e.g., in Ohio), and forest vegetation (New England and Nova Scotia). Additional measurements were performed during the transfer flights between Tampa, Florida, and Portsmouth on 5 July and 15 August 2004. During the study period, large forest fires were burning in Alaska and western Canada, and the fire plumes were regularly observed in the free troposphere over the northeastern United States [de Gouw et al., 2006; Pfister et al., 2005]. The forest fire emissions could easily be distinguished from urban emissions using acetonitrile (CH_3CN) as a tracer, and those data are excluded in this study [Warneke et al., 2006].

2.1.2. Ship

[9] Measurements were made on board the NOAA research ship Ronald H. Brown (RHB) during a cruise from 5 July until 12 August 2004, that started and ended in Portsmouth, New Hampshire. Most of the time was spent off the Massachusetts and New Hampshire coast and on a few occasions the ship went further north in the Gulf of Maine to sample more processed continental outflow. At various times, the sampled air was impacted by biogenic emissions [Quinn et al., 2006]. The forest fire plumes from Alaska and western Canada only rarely mixed down to the marine boundary layer and were a relatively minor component in the observations [Warneke et al., 2006].

2.2. Trace Gas Measurements

[10] VOC mixing ratios on board the WP-3D were measured by proton-transfer-reaction mass spectrometry (PTR-MS) [de Gouw and Warneke, 2007; de Gouw et al., 2006] and from gas chromatographic analyses of whole air samples (WAS) [Schauffler et al., 1999; Wert et al., 2003]. The PTR-MS stepped through a series of masses every ~17 s and the data have a calibration accuracy of ~15%. The measurement precision is determined by ion counting statistics and depends on the measured mixing ratios as discussed elsewhere [de Gouw and Warneke, 2007; de Gouw et al., 2006]. In this study, we use the measurement results for (1) benzene and toluene, (2) isoprene and the sum of its oxidation products methyl vinyl ketone and methacrolein (PTR-MS cannot separately measure these isomeric species), and (3) the sum of monoterpenes. The WAS samples were analyzed for more than 70 VOCs including alkanes, alkenes, acetylene, aromatics and several biogenic VOCs using a variety of separation and detection techniques. As many as 80 samples, collected over time intervals from 5 to 29 s (mean interval 10 s), were taken on most ~8 h flights, and were either automatically sampled at constant time intervals or triggered by a scientist on board the aircraft on the basis of conditions encountered in flight. This study will focus primarily on measurements of toluene, benzene and acetylene. Where possible, the PTR-MS and WAS measurements have been intercompared and were generally found to agree within the combined uncertainties [de Gouw and Warneke, 2007; de Gouw et al., 2006].

[11] On board the ship, VOCs were measured by online gas chromatography–mass spectrometry (GC-MS) [Goldan et al., 2004] and by proton-transfer ion trap mass spectrometry (PIT-MS) [Warneke et al., 2005]; only the GC-MS data for benzene and toluene are used in this study. Urban emission ratios of VOCs were determined from the GC-MS data set elsewhere [Warneke et al., 2007] and are used here in the discussion of the results.

[12] Carbon monoxide (CO) was measured on board the aircraft using a custom-built vacuum ultraviolet (VUV) fluorescence instrument with a response time of 1 s and an accuracy of 5% [Holloway et al., 2000]. On board the ship, CO was measured with a commercial VUV fluorescence instrument with an accuracy of 5% (Aerolaser GmbH) [Gerbig et al., 1999].

2.3. Particle Composition Measurements

2.3.1. Water-Soluble Organic Carbon

[13] The composition of submicron particles was measured on board both the ship and the aircraft using a particle-into-liquid sampler (PILS) with two online detectors to measure inorganic ionic constituents by ion chromatography (IC), and water-soluble organic carbon (WSOC) by a total organic carbon (TOC) analyzer [Sullivan et al., 2004]. In this study, we use results of the WSOC measurements only, which have a time resolution on the aircraft of ~1 min, and a combined uncertainty of $\pm (8\% + 0.3 \ \mu g \ C \ m^{-3})$. More details on the aircraft measurements have been given elsewhere [Peltier et al., 2007a, 2007b; Sullivan et al., 2006; Weber et al., 2007]. The TOC analyzer aboard the ship was run in the standard mode (ground-based mode [Sullivan et al., 2006]), which has a time resolution of 6 min. A particle filter was automatically switched in line for 15 min of every hour to establish the instrument background, i.e., the signal in the absence of particles.

2.3.2. Organic Matter

[14] Organic matter (OM), defined as the mass of organic compounds in aerosol particles with a diameter <1 μm, was measured both on board the ship and the aircraft using an Aerodyne aerosol mass spectrometer (AMS) with a quadrupole mass filter [Canagaratna et al., 2007; Jayne et al., 2000]. More details on the ship measurements have been given elsewhere [Quinn et al., 2006].

[15] On board the aircraft, the AMS and PILS instruments sampled air from the University of Denver low-turbulence inlet (LTI) that had passed through a single-stage micro-orifice uniform deposition impactor (Model 100, MSP Corp.) with a nominal 50% cut point at an aerodynamic diameter of 1.0 μm. The AMS used a pressure-controlled inlet to reduce the sample line pressure to a constant value in front of the aerodynamic lens system in the instrument (R. Bahreini et al., Design and operation of a pressure controlled inlet for airborne sampling with an aerodynamic lens, submitted to Aerosol Science and Technology, 2007). This combination of inlets resulted in a sampling efficiency that was independent of altitude, but that was low relative to previous ground-based operation of the instrument. The particle transmission efficiency as a function of size of the combined system was characterized (Bahreini et al., submitted manuscript, 2007) and used to correct the measured size distributions. Particles from 0.06 to 0.7 μm vacuum aerodynamic diameter, or ~0.04 to ~0.5 μm physical diameter, were transmitted through the AMS inlet system with quantifiable efficiency; however, the integrated correction factor for particle transmission losses was significant and typically between 2 and 3.25 (or integrated particle

transmission of 0.3–0.5). Since the volume-weighted distribution of physical diameters extended above 0.4 μm in some cases, the airborne AMS may be expected to underreport particle mass in these cases. Particle bounce off the vaporizer can also affect the AMS collection efficiency. For the shipboard measurements, this collection efficiency was determined by comparisons of the AMS sulfate with PILS-IC sulfate and ranged from 0.45 to 1 depending on acidity [*Quinn et al.*, 2006]. After accounting for particle transmission losses from the inlet system and applying an average collection efficiency of 0.75 for particle bounce [*Allan et al.*, 2004; *de Gouw et al.*, 2005; *Quinn et al.*, 2006], the correlation for 10-min averaged airborne AMS sulfate data with the airborne PILS-IC sulfate was linear forced through zero with a slope of 1.0 and a correlation coefficient (r^2) of 0.8. Although mass spectra and particle time-of-flight data were recorded every 30 s, signal-to-noise was generally poor for aircraft operation of the quadrupole AMS [*Bahreini et al.*, 2003] and averaging periods of 10 min were needed for this data set. The detection limit of the 10-min averages for nonrefractory organics was 0.6 μg m^{-3} and the precision was ∼45%, on the basis of the AMS sulfate correlation with PILS-IC sulfate.

2.3.3. Organic Carbon

[16] On board the ship, organic carbon (OC) and elemental carbon (EC) were sampled in both the sub- and super-μm size ranges using different combinations of impactors, filters and denuders [*Bates et al.*, 2005; *Mader et al.*, 2003; *Schauer et al.*, 2003]. During ICARTT an additional semicontinuous, real-time carbon aerosol analysis instrument (Sunset Laboratory Field Instrument) was used to increase the time resolution of OC sampling (45 or 105 min depending on the OC concentrations). The data reported here were collected with the semicontinuous instrument. Sources of uncertainty for the semicontinuous real-time OC measurement include the air volume sampled (5%) and the precision of the method (3%) based on injection of a CH$_4$ standard with each run. The total uncertainty, calculated as the sum of the squares, was 6%.

2.3.4. Comparison Between the Aerosol Organics Measurements

[17] The OM, OC and WSOC measurements all quantify different aspects of the organic aerosol. What can be learned about the organic aerosol from the comparison? A literature survey has indicated that OM/OC ratios range from 1.6 μg μg C^{-1} for urban aerosol to 2.1 μg μg C^{-1} for rural aerosol [*Turpin and Lim*, 2001], as a result of photochemical processing. A study in Pittsburgh indicated that OM/OC ratios are lower (1.2 μg μg C^{-1}) for hydrocarbon-like aerosol [*Zhang et al.*, 2005b]. Figure 1a shows a scatterplot of OM versus OC measured on board the ship. The two measurements were linearly correlated with a least squares correlation coefficient (r^2) of 0.69 and a slope of 1.95 μg μg C^{-1}. (The fits in Figures 1a, 1c, and 1e have been forced through zero, because we are mostly interested in comparing the measurement ratios to other results in the literature. For the data in Figures 1a and 1c, leaving the intercept as a free parameter in the fit did not make a significant difference; for the data in Figure 1e an intercept of about 0.8–1.0 μg m^{-3} in OM is found.) Within the uncertainties, the latter value agrees with the ratio of 1.78 μg μg C^{-1} determined previously for measurements in the Gulf of

Maine [*de Gouw et al.*, 2005]. The measured data span a wider range of OM/OC ratios than given in the literature [*Turpin and Lim*, 2001] as indicated by the shaded area in Figure 1a. Figure 1b shows a histogram of the observed OM/OC ratios, which ranged from roughly 1 to 3 μg μg C^{-1}.

[18] The ratio between WSOC and OC in an air mass increases with photochemical processing, and was found to range between 0.4 and 0.8 μg C μg C^{-1} during an urban study in St. Louis [*Sullivan et al.*, 2004]. Figure 1c shows a scatterplot of WSOC versus OC measured on board the ship. The two measurements correlated well with $r^2 = 0.86$ and the slope of a linear fit to the data is 0.55 μg C μg C^{-1}. The measured data lie in the 0.4–0.8 μg C μg C^{-1} range indicated by the shaded area in Figure 1c. The histogram of observed WSOC/OC ratio (Figure 1d) shows a range of values between 0.4 and 0.7 μg C μg C^{-1}. There are several indications in the literature that primary, urban emissions of WSOC are negligibly small [*Huang and Yu*, 2007; *Huang et al.*, 2006; *Weber et al.*, 2007]. It should be noted, however, that zero WSOC/OC ratios were not observed on the ship, in accord with the fact that air masses with primary emissions only were not sampled.

[19] Figure 1e shows scatterplots of OM versus WSOC for both the ship and aircraft data. The linear correlation coefficient (r^2) between the two measurements is 0.60 for the ship data and 0.57 for the aircraft data. We look at OM/WSOC ratios here for conversion of the WSOC data, which are an operationally defined parameter, into estimates for OM, i.e., an atmospherically relevant parameter, in the companion paper [*Brock et al.*, 2008]. The OM/WSOC ratios were significantly higher on the ship in comparison with the aircraft: the slope of a linear fit to the data in Figure 1e is 3.3 μg μg C^{-1} for the ship data and 2.0 μg μg C^{-1} for the aircraft data. The reason for this difference is unknown, but more likely due to the combined uncertainties of the measurements involved than to a real atmospheric difference. The shaded area in Figure 1e represents the range of values calculated from the ranges in OM/OC (1.6–2.1 μg μg C^{-1}) and in WSOC/OC (0.4–0.8 μg C μg C^{-1}). This may be an overestimate of the range in OM/WSOC, since OM/OC and WSOC/OC ratios are not independent from each other: primary, urban aerosol has both a low OM/OC and WSOC/OC ratio, whereas the opposite is true for processed, urban aerosol. Nevertheless, the shaded area in Figure 1e describes the range in observed OM/WSOC ratios on board the ship very well; the data from the aircraft are at the low end and below this range. The histogram of OM/WSOC ratios in Figure 1f shows a wide range from roughly 2 to 6 μg μg C^{-1}. An average OM/WSOC ratio of 2.8 was determined from all data (aircraft and ship) for use in the companion paper [*Brock et al.*, 2008], and is indicated by the dotted lines in Figures 1e and 1f.

3. Semiempirical Description of OM, OC, and WSOC in Urban Plumes

[20] In an earlier paper, we derived a semiempirical relationship between the ratio $\Delta OM/\Delta C_2H_2$ and the photochemical age, Δt, of urban plumes [*de Gouw et al.*, 2005]. This relationship is described in detail in section 3.1. The central question in this study is how well this relationship describes the data obtained during ICARTT. To facilitate
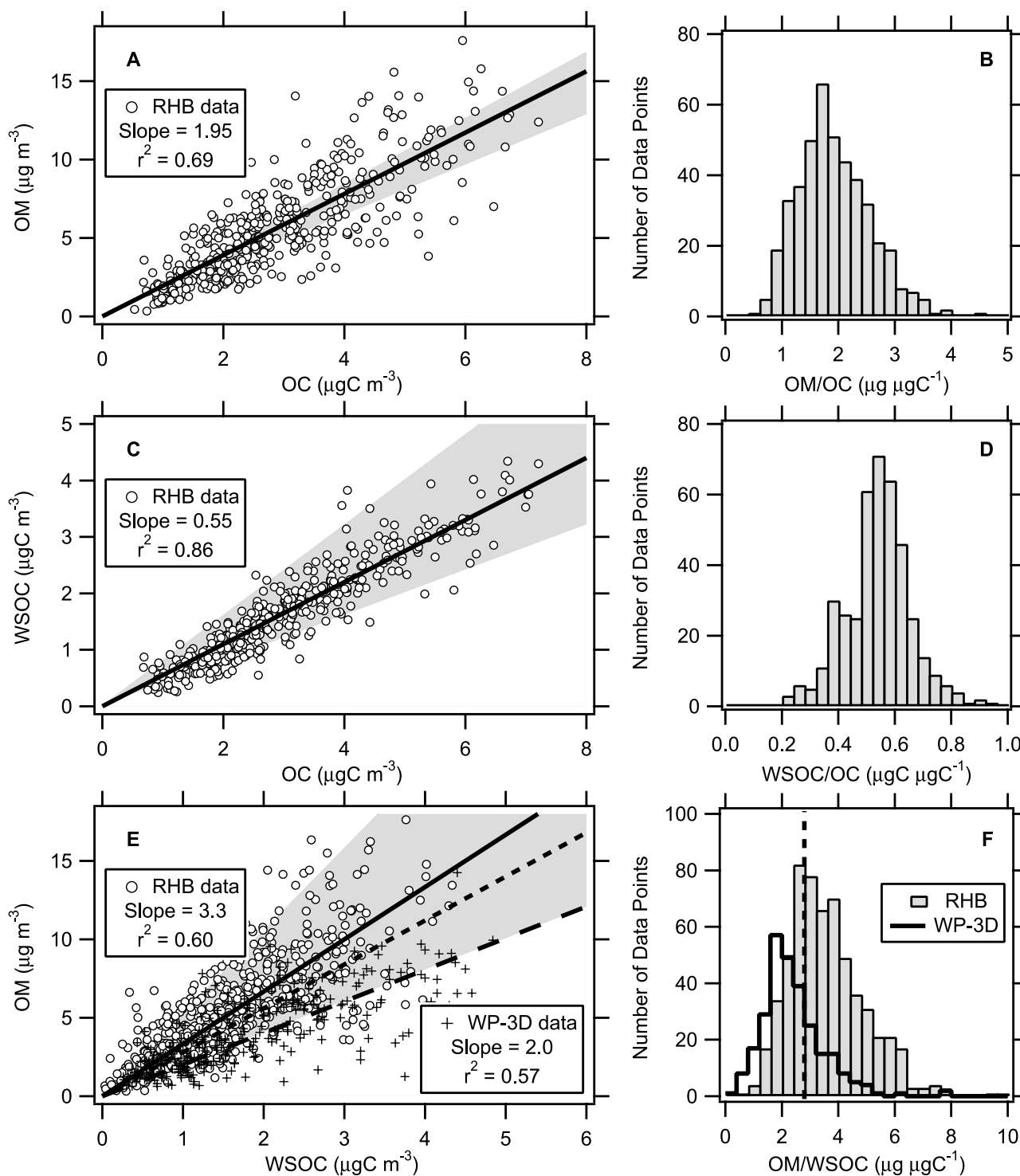
Figure 1. (a–f) Comparison between the OM, OC and WSOC measurements on board the research ship *Ronald H. Brown* (RHB) and the WP-3D research aircraft. The open circles in Figures 1a, 1c and 1e show data from the ship, whereas the crosses in Figure 1e show data from the aircraft. The shaded areas in Figures 1a, 1c and 1e show the range of values described in the literature. Figures 1b, 1d and 1f show histograms of the measured OM/OC, WSOC/OC and OM/WSOC ratios, respectively. The average relationship OM = 2.8 × WSOC, derived from all data, is shown by the dashed lines in Figures 1e and 1f.

this comparison, however, we convert the $\Delta OM/\Delta C_2H_2$ ratio to $\Delta OM/\Delta CO$, $\Delta OC/\Delta CO$ and $\Delta WSOC/\Delta CO$ ratios in section 3.2. We end this chapter by describing in section 3.3 how much formation of secondary OM can be expected in an urban plume from the known emissions of urban VOCs. The results from chapter 3 will be needed in chapter 4 for comparison with the observations from ICARTT.

3.1. $\Delta OM/\Delta C_2H_2$ Versus Photochemical Age: A Semiempirical Relationship From NEAQS 2002

[21] From the NEAQS 2002 study, a relationship between the ratio $\Delta OM/\Delta C_2H_2$ and the photochemical age, Δt, of urban plumes was derived, which explained a significant part of the variance in the OM data [*de Gouw et al.*, 2005]:

$$
\begin{aligned}
\frac{\Delta OM}{\Delta C_2H_2} = {}& ER_{OM} \times \frac{\exp(-L_{OM}\Delta t)}{\exp(-k_{C_2H_2}[OH]\Delta t)} \\
& + ER_{precursor} \times Y_{OM} \times \frac{P_{OM}}{L_{OM} - P_{OM}} \\
& \times \frac{\exp(-P_{OM}\Delta t) - \exp(-L_{OM}\Delta t)}{\exp(-k_{C_2H_2}[OH]\Delta t)}.
\end{aligned} \tag{1}
$$

In this equation, the parameter ER_{OM} is the emission ratio versus acetylene of primary OM, $ER_{precursor}$ is the emission ratio versus acetylene of the precursors of secondary OM, Y_{OM} is the yield for the precursors to produce OM, and L_{OM} and P_{OM} are the loss and formation rate of OM, respectively. The production rate P_{OM} equals the loss rate, $k_{precursor}[OH]$, of its precursors versus OH. Furthermore, $k_{C_2H_2}$ is the rate coefficient for the C_2H_2 + OH reaction, and [OH] is the 24-h average OH concentration (3×10^6 molecules cm^{-3} [*de Gouw et al.*, 2005]).

[22] The first line in equation (1) represented the direct emissions of OM and their removal. The second line represented the secondary formation from the available precursors and the removal of the secondary OM (note that the loss rates of primary and secondary OM are the same in equation (1)). It was assumed in equation (1) that the formation of secondary OM from all precursors combined can be described by an average rate (P_{OM}) and average yield (Y_{OM}), which is obviously a simplification. A more detailed description should also include the effects of aerosol volatility, i.e., the fact that aerosol yields increase with total mass loading, and the formation of OM from first-generation products of VOCs, which leads to a delayed onset of secondary OM formation [*Donahue et al.*, 2006]. It was furthermore assumed in equation (1) that wet deposition of OM is a negligible loss process; wet deposition would lead to a decoupling of the aerosol and gas-phase properties of an urban air mass, and a treatment such as presented by equation (1) would cease to be valid.

[23] The photochemical age (Δt) in equation (1) was defined as:

$$
\begin{aligned}
\Delta t = {}& \frac{1}{[OH](k_{toluene} - k_{benzene})} \times \left[\ln\left(\left. \frac{[toluene]}{[benzene]} \right|_{t=0} \right) \right. \\
& \left. - \ln\left(\frac{[toluene]}{[benzene]} \right) \right],
\end{aligned} \tag{2}
$$

where $k_{toluene}$ and $k_{benzene}$ are the rate coefficients for the reaction of OH with toluene (5.63×10^{-12} cm^3 molecule^{-1} s^{-1}) and benzene (1.22×10^{-12} cm^3 molecule^{-1} s^{-1}) [*Atkinson and Arey*, 2003], and [toluene]/[benzene]$|_{t=0}$ is the toluene/benzene ratio at the source (3.7 [*de Gouw et al.*, 2005]).

[24] From the NEAQS 2002 data, the following values were found for the parameters in equation (1) by fitting the equation to the observations [*de Gouw et al.*, 2005]:

$$ ER_{OM} = 1.9 \, \mu g \, m^{-3} \, ppbv^{-1} $$

$$ ER_{precursor} \times Y_{OM} = 17 \, \mu g \, m^{-3} \, ppbv^{-1} $$

$$ L_{OM} = 0.00677 \, h^{-1} $$

$$ P_{OM} = 0.0384 \, h^{-1} $$

(the parameters $ER_{precursor}$ and Y_{OM} are coupled in equation (1) and only the product was determined). The loss and formation rates of OM correspond to atmospheric lifetimes for OM and its precursors of approximately 6 and 1 d, respectively, which is in the range of expected values [*Maria et al.*, 2004].

3.2. Conversion of the NEAQS Relationship

[25] We will now convert the parameterization of $\Delta OM/\Delta C_2H_2$ versus photochemical age derived in our earlier work [*de Gouw et al.*, 2005], i.e., equation (1), to $\Delta OM/\Delta CO$, $\Delta OC/\Delta CO$ and $\Delta WSOC/\Delta CO$ ratios in order to facilitate comparison with the data obtained during ICARTT.

3.2.1. $\Delta OM/\Delta CO$ Versus Photochemical Age

[26] Acetylene was used in equation (1) because data for carbon monoxide (CO), a more universally measured tracer of urban pollution, were not available during NEAQS 2002. To convert equation (1) to $\Delta OM/\Delta CO$ ratios we use here:

$$
\begin{aligned}
\frac{\Delta C_2H_2}{\Delta CO} & = ER_{C_2H_2} \times \exp(-(k_{C_2H_2} - k_{CO})[OH]\Delta t) \\
& \approx ER_{C_2H_2} \times \exp(-k_{C_2H_2}[OH]\Delta t),
\end{aligned} \tag{3}
$$

where $ER_{C_2H_2}$ is the emission ratio of acetylene versus carbon monoxide (CO). Secondary formation of CO from anthropogenic VOCs is assumed to be zero in equation (3), which is likely a good assumption: secondary CO from anthropogenic VOCs was estimated to be only 1% of the total CO close to emission sources in Los Angeles [*Griffin et al.*, 2007]. The approximation on the right-hand side of equation (3) is made because $k_{C_2H_2} \gg k_{CO}$; that is, the loss of CO is negligible on a timescale of several days that is relevant to the formation and loss of OM. Using (3), equation (1) can be rewritten as:

$$
\begin{aligned}
\frac{\Delta OM}{\Delta CO} = {}& ER'_{OM} \times \exp(-L_{OM}\Delta t) \\
& + ER'_{precursor} \times Y_{OM} \times \frac{P_{OM}}{L_{OM} - P_{OM}} \\
& \times (\exp(-P_{OM}\Delta t) - \exp(-L_{OM}\Delta t)),
\end{aligned} \tag{4}
$$

where the primed emission ratios, ER'_{OM} and $ER'_{precursor}$, indicate that the emissions are now ratioed versus CO.
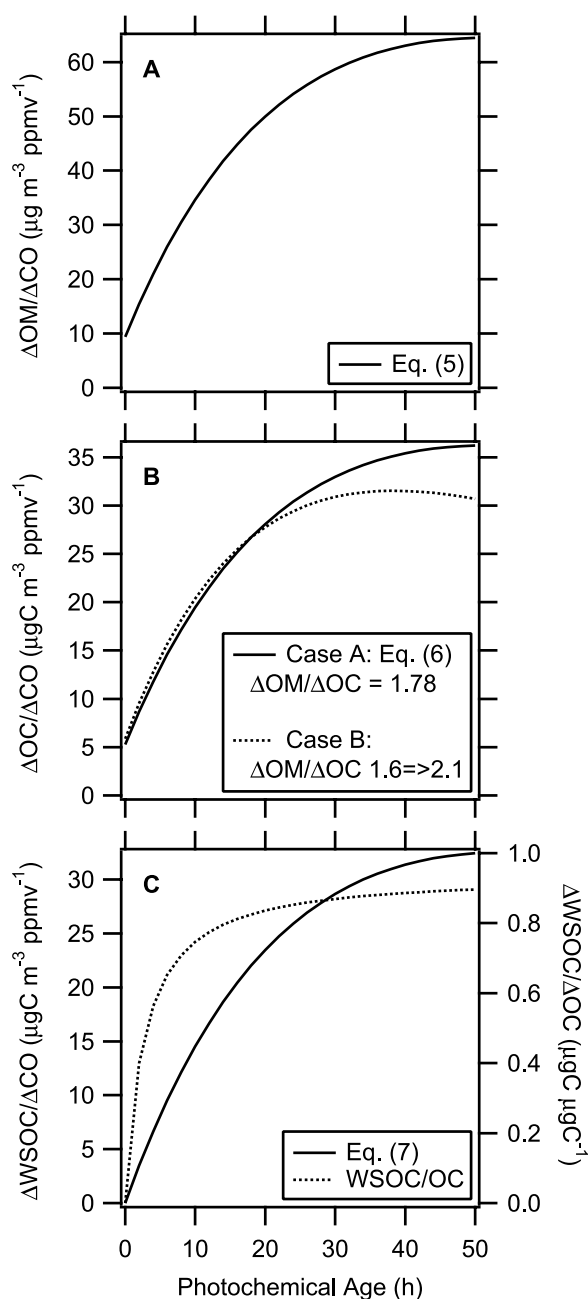
Figure 2. Evolution of (a) OM, (b) OC and (c) WSOC in urban air. See the text for an explanation of the different curves.

Using $ER_{C_2H_2} = 4.94$ ppbv ppmv^{-1} [*de Gouw et al.*, 2005], these parameters are:

$$ER'_{OM} = 9.4\,\mu g\,m^{-3}\,ppmv^{-1}$$

$$ER'_{precursor} \times Y_{OM} = 84\,\mu g\,m^{-3}\,ppmv^{-1}.$$

[27] The value for ER'_{OM} is in the range of values observed in Zurich (10.4 $\mu g\,m^{-3}$ ppmv^{-1}) [*Lanz et al.*, 2006] and Tokyo (11 $\mu g\,m^{-3}$ ppmv^{-1}) [*Takegawa et al.*, 2006b], but higher than the values expected for vehicle

exhaust: a $\Delta OC/\Delta CO$ ratio of 2.1 $\mu g\,C\,m^{-3}$ ppmv^{-1} was determined from a tunnel study [*Kirchstetter et al.*, 1999], which corresponds to a $\Delta OM/\Delta CO$ of approximately 3.4 $\mu g\,m^{-3}$ ppmv^{-1} assuming a $\Delta OM/\Delta OC$ ratio of 1.6 $\mu g\,\mu g\,C^{-1}$ for primary aerosol [*Turpin and Lim*, 2001]. The tunnel data are in better agreement with the ratio between HOA (hydrocarbon-like organic aerosol) and CO of 4.3 $\mu g\,m^{-3}$ ppmv^{-1} in Pittsburgh [*Zhang et al.*, 2005b]. The difference between our estimate of the urban emission ratio and the ratio for vehicle exhaust may be explained by (1) the fact that there are more primary OM sources in cities than just vehicles [*Schauer and Cass*, 2000; *Schauer et al.*, 1996] and (2) our previous data treatment may overestimate the primary emissions of OM, because it is difficult to account for rapid OM growth in urban air when sampling from a platform that is outside the city. Also, the tunnel study that determined the $\Delta OC/\Delta CO$ ratio was conducted in 1997 in California and vehicle emissions have significantly changed over the last decade [*Parrish*, 2006] and may also be regionally different.

[28] Using the above values of ER'_{OM}, $ER'_{precursor}$, L_{OM} and P_{OM}, we can write for $\Delta OM/\Delta CO$ ratio (in $\mu g\,m^{-3}$ ppmv^{-1}) as a function of photochemical age (in h):

$$\frac{\Delta OM}{\Delta CO} = 9.4 \times \exp(-0.00677 \times \Delta t) + 102$$
$$\times (\exp(-0.00677 \times \Delta t) - \exp(-0.0384 \times \Delta t)). \quad (5)$$

The $\Delta OM/\Delta CO$ ratio calculated according to equation (5) is shown in Figure 2a. The ratio increases by more than a factor of 6 going from 0 to a 50-h photochemical age.

3.2.2. $\Delta OC/\Delta CO$ Versus Photochemical Age

[29] The concentration of OM (the total mass of organic compounds in particulate matter) and of OC (the total mass of particulate organic carbon) are measured by independent techniques. The $\Delta OM/\Delta OC$ ratio ranges from 1.6 $\mu g\,\mu g\,C^{-1}$ for urban aerosol to 2.1 $\mu g\,\mu g\,C^{-1}$ for rural aerosol [*Turpin and Lim*, 2001], which brackets the average value of 1.78 $\mu g\,\mu g\,C^{-1}$ determined previously for the northeastern United States [*de Gouw et al.*, 2005]. Figure 2b shows the $\Delta OC/\Delta CO$ ratio as a function of age calculated for two cases: case A assumes equation (5) and a constant $\Delta OM/\Delta OC$ ratio of 1.78 $\mu g\,\mu g\,C^{-1}$; case B assumes equation (5) and a $\Delta OM/\Delta OC$ ratio that increases linearly with age from 1.6 (at $\Delta t = 0$) to 2.1 $\mu g\,\mu g\,C^{-1}$ (at $\Delta t = 50$ h). Figure 2b shows that the two calculated curves are very similar in the first 24 h; after that they diverge by up to 20%. For reasons of simplicity, we assume a constant $\Delta OM/\Delta OC$ of 1.78 $\mu g\,\mu g\,C^{-1}$; using this assumption equation (5) can be converted to describe the $\Delta OC/\Delta CO$ ratio (in $\mu g\,C\,m^{-3}$ ppmv^{-1}) as a function of photochemical age (in h):

$$\frac{\Delta OC}{\Delta CO} = 5.3 \times \exp(-0.00677 \times \Delta t) + 57$$
$$\times (\exp(-0.00677 \times \Delta t) - \exp(-0.0384 \times \Delta t)). \quad (6)$$

3.2.3. $\Delta WSOC/\Delta CO$ Versus Photochemical Age

[30] There are several indications in the literature that primary emissions of WSOC are negligibly small [*Huang and Yu*, 2007; *Huang et al.*, 2006; *Weber et al.*, 2007]. If we furthermore assume that all secondary OC is water

soluble [*Kondo et al.*, 2007], then the ΔWSOC/ΔCO ratio (in μg C m^{-3} ppmv^{-1}) as a function of age (in h) is given by the second term in equation (6), i.e.,

$$\frac{\Delta\text{WSOC}}{\Delta\text{CO}} = 57 \times (\exp(-0.00677 \times \Delta t) - \exp(-0.0384 \times \Delta t)). \tag{7}$$

The ΔWSOC/ΔCO ratio calculated using equation (7) is shown in Figure 2c along with the ΔWSOC/ΔOC ratio calculated using equations (6) and (7). The calculation suggests that after emission the water-soluble fraction of OC increases rapidly from zero to 0.84 μg C μg C^{-1} at 10 h of processing, and then increases more slowly to about 0.90 μg C μg C^{-1} after 2 d.

3.3. Secondary Formation From Urban VOCs

[31] The formation of OM in urban plumes can be estimated using a bottom-up approach from measured emission ratios of gas-phase precursors ($ER'_{precursor}$) and the yields for secondary formation derived from smog chamber studies (Y_{OM}). Previously, we have shown that the secondary formation expected from commonly measured precursors is small in comparison with the increase in OM observed in urban plumes [*de Gouw et al.*, 2005]. Since then, new experiments have demonstrated that particulate yields for aromatic species can be much higher in low-NOx conditions [*Ng et al.*, 2007b], and we investigate the implications in this work.

[32] A method to estimate VOC emission ratios ($ER'_{precursor}$) has been described elsewhere and involves (1) graphing the ratio of VOCs versus an inert tracer (e.g., acetylene or CO) as a function of the photochemical age (equation (2)) and (2) extrapolating the ratio to a zero photochemical age [*de Gouw et al.*, 2005; *Warneke et al.*, 2007]. The VOC emission ratios calculated from the 2002 and 2004 studies in the northeastern United States are shown in Figure 3a and were very similar between the 2 years. Not included in Figure 3 are several oxygenated VOCs such as the small aldehydes (C_2-C_3), ketones (C_3-C_4), alcohols (C_1-C_2) and acids (C_1-C_2). These species were measured but are omitted from the discussion, because (1) it is more difficult to estimate their urban emission ratios, since they can have primary, secondary and biogenic sources [*de Gouw et al.*, 2005], and (2) the particulate yields of the measured, oxygenated VOCs have been measured to be zero [*Seinfeld and Pandis*, 1998].

[33] Particulate yields (Y_{OM}) have been published for most of the VOCs in Figure 3b, and are zero for the small alkanes and alkenes, low for the higher ($>C_8$) and cyclic alkanes, and the highest for aromatic compounds [*Seinfeld and Pandis*, 1998]. Also included in Figure 3b are new results for benzene, toluene and m-xylene in low-NOx conditions [*Ng et al.*, 2007b], which are significantly higher than previous results.

[34] The product of the VOC emission ratios and the particulate yields gives the maximum formation of OM per CO emitted ($ER'_{precursor} \times Y_{OM}$; Figure 3c); that is, the OM formed after all of a particular VOC has reacted and in the absence of OM losses. In this analysis, the highest contributions of secondary OM comes from toluene, which has both one of the higher emission ratios and particulate yields.

The maximum contributions from all VOCs add up 3.7 μg m^{-3} ppmv^{-1} when using the yields from *Seinfeld and Pandis* [1998]. This number is smaller than the ΔOM/ΔCO ratio for primary, urban emissions (9.4 μg m^{-3} ppmv^{-1}) and much smaller than the ΔOM/ΔCO ratios of over 60 μg m^{-3} ppmv^{-1} in aged, urban plumes (Figure 2a). For this reason, the growth of secondary OM could not be explained using the particulate yields of *Seinfeld and Pandis* [1998], which was one of the main findings in our previous study [*de Gouw et al.*, 2005]. Newly published particulate yields from Seinfeld and coworkers [*Ng et al.*, 2007b] are significantly higher in conditions with low NOx (<1 ppbv), which are much closer to actual ambient conditions in urban plumes (NOx mixing ratios between 1 and 10 ppbv [*Neuman et al.*, 2006]) than high-NOx (~1 ppmv) conditions. (The ratio between NO and HO$_2$ is what really determines the similarities between the smog chamber simulations and the ambient atmosphere, as it controls the relative importance of the reactions forming organic peroxides and nitrates.) If we assume that the particulate yield is 34% (the average for benzene, toluene and m-xylene) for the aromatic species not studied by *Ng et al.* [2007b], then the contributions from all VOCs add up to 14.1 μg m^{-3} ppmv^{-1}. This number is approximately 4 times greater than the previous result and, combined with the primary emissions of OM that we have estimated, amounts to a maximum ΔOM/ΔCO ratio of 23.5 μg m^{-3} ppmv^{-1}. The ΔOM/ΔCO ratios estimated from the known emissions of VOCs are compared to the observations from ICARTT in the next chapter.

4. Results

[35] In this chapter we present results from the organic aerosol measurements during ICARTT, and study in particular how well the semiempirical relationships discussed in the previous chapter describe the data for OM and WSOC obtained on board the research ship *Ronald H. Brown* and WP-3D aircraft.

4.1. Ship-Based Measurements of OM

[36] The OM and CO data from the entire ship cruise of the *Ronald H. Brown* (Figure 4a) were correlated with a linear correlation coefficient (r^2) of 0.49 (Figure 4b). The slope of a linear fit to all data is 41 ± 5 μg m^{-3} ppmv^{-1}. Part of the scatter is explained by the secondary formation of OM described by equation (5). To illustrate this point, the data points in Figure 4b are color-coded by the photochemical age determined by equation (2). It is seen that the data with a higher photochemical age (black points) tend to follow a steeper line than the points with a lower photochemical age (yellow points). The stratification of data is not as clear as was the case during the 2002 New England Air Quality Study [*de Gouw et al.*, 2005], probably because unprocessed air masses were not encountered as frequently in 2004. Using equation (5) the ΔOM/ΔCO ratios after 24 and 48 h are calculated and are shown by the solid and dashed blue lines in Figure 4b. Most of the data points follow the 24- and 48-h lines, which means that the results from ICARTT are consistent with those from NEAQS 2002. Also shown in Figure 4b are (1) the ratio of 9.4 μg m^{-3} ppmv^{-1} for primary urban emissions (solid black line) and
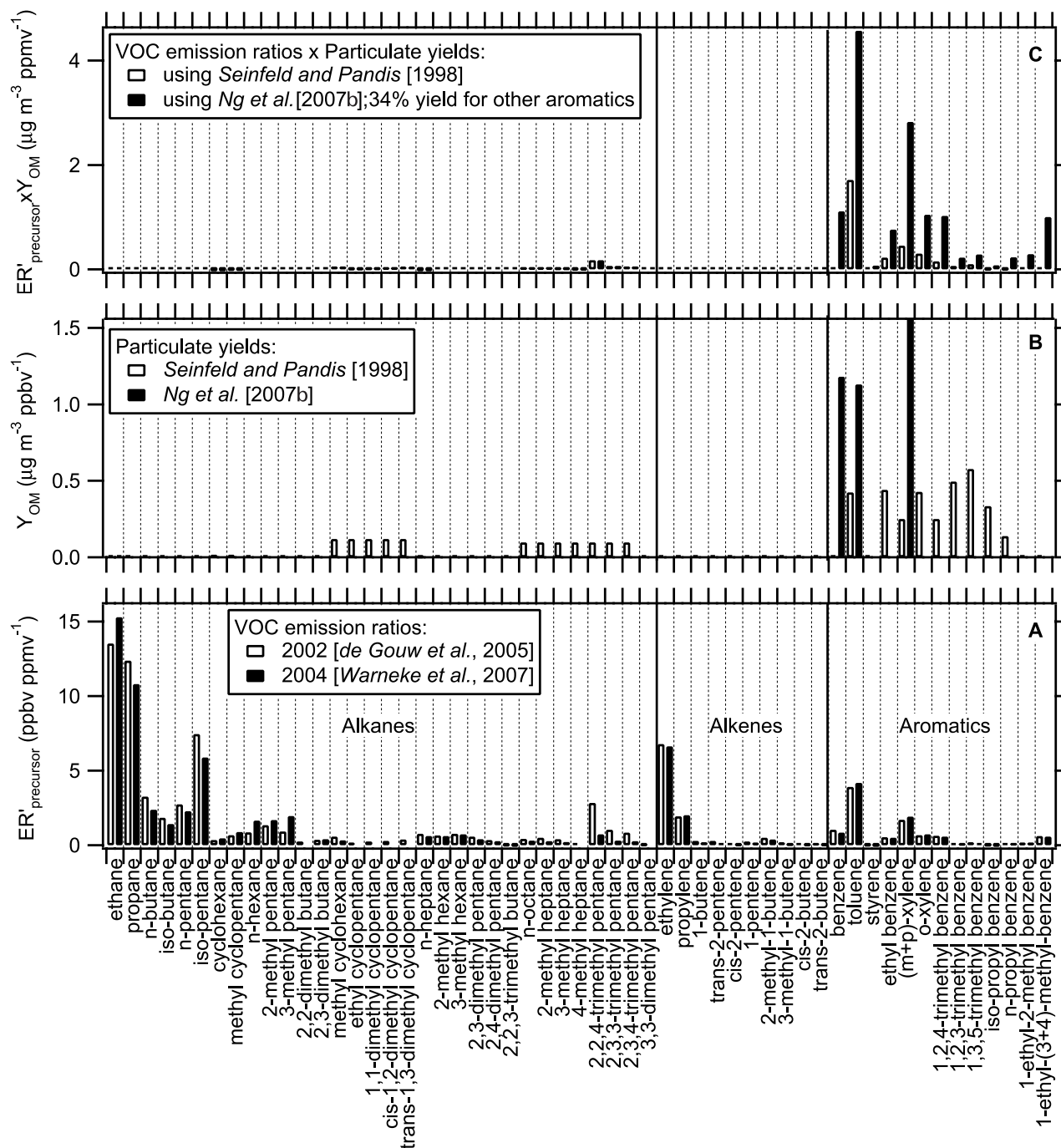
Figure 3. Urban emissions of VOCs and their potential to form OM. (a) The VOC emission ratios versus CO determined from the GC-MS measurements on board the *Ronald H. Brown* in 2002 and 2004. (b) Published and estimated particulate yields for all measured VOCs. (c) The product of the numbers in Figure 3a (average of 2002 and 2004 results) and Figure 3b.

(2) the ratio of 9.4 + 14.1 = 23.5 $\mu g\ m^{-3}\ ppmv^{-1}$ for primary emissions plus secondary formation according to the yields from *Ng et al.* [2007b] as described in section 3.3 (dotted black line). Only a few points lie along the primary emissions line; that is, only a few air masses were observed with a low degree of photochemical processing. The line calculated using the results from *Ng et al.* [2007b] is at the low end of the observed range in data points. The average $\Delta OM/\Delta CO$ ratio for all data points with a photochemical

age above 1 d is 47 ± 7 $\mu g\ m^{-3}\ ppmv^{-1}$. Relative to the primary emissions, this represents a 1-d increase due to secondary formation of 38 ± 7 $\mu g\ m^{-3}\ ppmv^{-1}$. As discussed in section 3.3, the measured VOC precursors and the particulate yields of *Ng et al.* [2007b] account for 14.1 $\mu g\ m^{-3}\ ppmv^{-1}$ or 37% of this increase in OM.

[37] Equation (5), derived from the NEAQS 2002 data set [*de Gouw et al.*, 2005], was used to calculate the time series of OM measured in 2004 on board the *Ronald H. Brown*
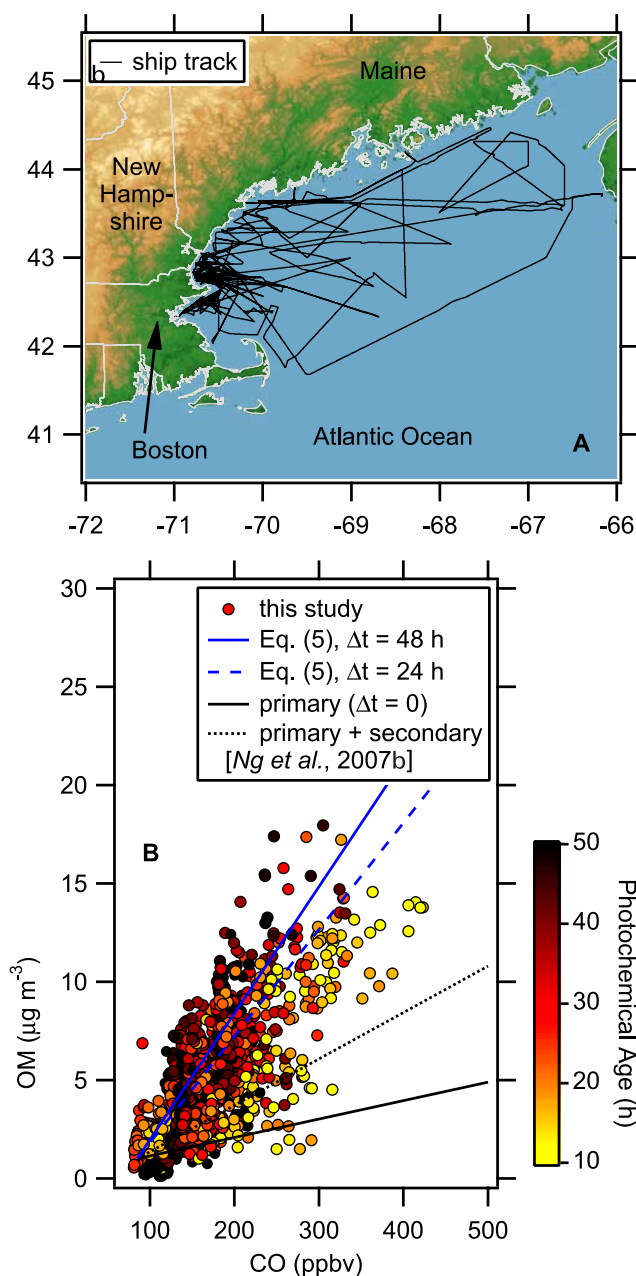
Figure 4. Measurement results for OM and CO obtained from the research ship *Ronald H. Brown*. (a) The cruise track and (b) a scatterplot of OM versus CO color-coded by the photochemical age according to equation (2). ΔOM/ΔCO ratios are calculated according to equation (5) and are shown for processing times of 24 and 48 h, respectively. Also indicated are the ΔOM/ΔCO ratio estimated for primary, urban emissions (solid black line), and the maximum ΔOM/ΔCO ratio calculated from the measured precursors (Figure 3) (dotted black line).

using the measured data for CO, benzene and toluene, and the results are shown in Figure 5a. The calculation closely follows the measured OM concentrations. It should be noted that this is not a fit of equation (5) to the data: Figure 5 compares data from ICARTT in 2004 with a semiempirical relationship derived from data from an earlier study in the

northeastern United States in 2002 [*de Gouw et al.*, 2005]. The good agreement suggests (1) that the observations were consistent between the 2 years and (2) that much of the observed variability in OM during ICARTT can be explained by secondary formation in urban plumes. Calculated and measured OM concentrations are correlated with a linear correlation coefficient of 0.59 (Figure 5b), which is higher than the 0.49 for the correlation between OM and CO in Figure 4b. The slope from a linear least squares fit to the data (Figure 5b) is slightly less than 1 at 0.86; the difference of 14% is well within the combined uncertainties in AMS data sets from different years and the uncertainty in the conversion from emission ratios versus acetylene to ratios versus CO (equation 3).

[38] The measurement of CO is used in this work as an indicator of urban emissions, and the good OM-CO and WSOC-CO correlations therefore suggest that the OM and WSOC sources are also related to urban emissions [*Sullivan et al.*, 2006]. The airborne observations in urban plumes will be the focus of the next 2 sections. After that, the limitations of using CO as an indicator of urban emissions, notably the fact that it can be formed in the photo-oxidation of methane and VOCs [*Granier et al.*, 2000], will be discussed.

4.2. Growth of WSOC in New York City Plume

[39] Measurements downwind of New York City (NYC) on two consecutive days, 20 and 21 July 2004, illustrate the growth of WSOC relative to CO as a result of photochemical processing (Figure 6). The data from these flights are unique and particularly useful because, after crossing Long Island, the NYC urban plume was advected above the stable marine boundary layer with no interaction with the ocean surface, no chemical processing by clouds and no influence from precipitation. Thus, the chemical evolution over transport periods of as much as 2 d could be evaluated without the confounding effects of additional sources or depositional losses.

[40] On 20 July, CO mixing ratios up to 400 ppbv were observed over Long Island, and on 21 July, CO levels over 300 ppbv were observed further east over the Atlantic Ocean (Figure 6a). Back trajectories from the locations of the highest anthropogenic CO observed on 20 and 21 July indicate that the sampled air came in both cases from the NYC area (Figure 6a). The back trajectories also indicate that the urban plume observed on 21 July was, 24 h earlier, very close to the location of the plume observed on 20 July. The combination of measurements on 20 and 21 July may not have been a true Lagrangian experiment, but the trajectory analysis does show that the aircraft sampled urban air masses from approximately the same area after very different processing times.

[41] The data for WSOC and CO were well correlated on both days (Figure 6b). Scatterplots of WSOC versus CO for both plume intercepts (Figure 7a) show that the ΔWSOC/ΔCO ratio, determined from the slopes of linear regressions to the data, was more than a factor of 2 higher on 21 July, indicating more WSOC per CO emitted following a day of photochemical processing (Table 2). Note that the ΔWSOC/ΔCO ratios on both days are higher than the primary emissions of OC according to equation (6) (5.3 μg C m^{-3} ppmv^{-1}) and much higher than the ΔOC/ΔCO ratio from a
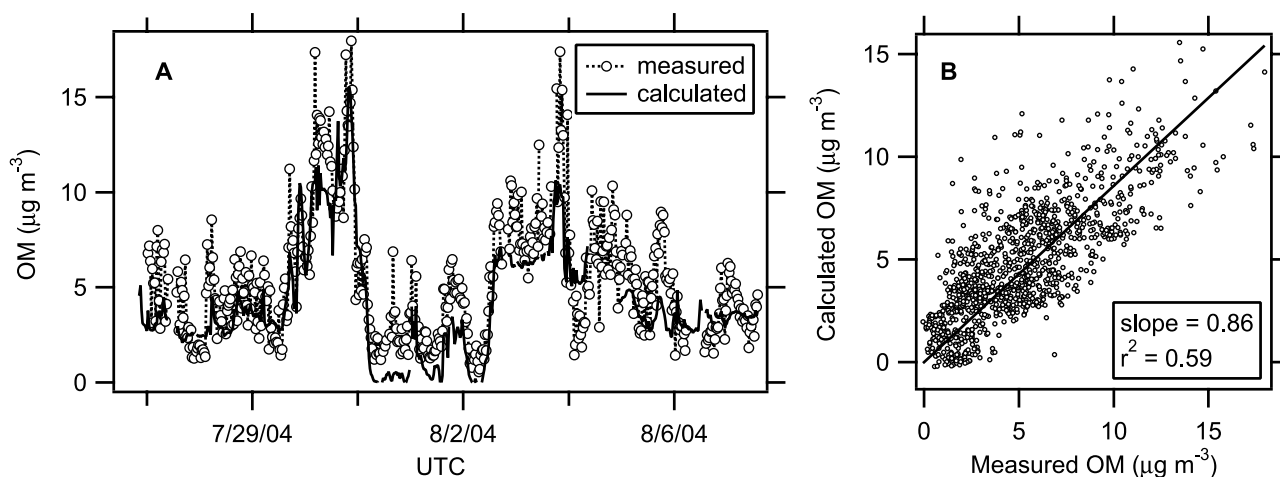
Figure 5. Comparison between the measured OM on board the *Ronald H. Brown* and the OM calculated according to equation (5). (a) A time series of part of the data and (b) a scatterplot of the entire data set.

tunnel study (2.1 μg C m^{-3} ppmv^{-1}) [*Kirchstetter et al.*, 1999]: it is therefore much more likely that the WSOC observed on 20 and 21 July came from secondary formation than from oxidation of primary emissions.

[42] Toluene and benzene, also present in the NYC plume (Figure 6c), are oxidized in the gas phase by OH; however, toluene is the more reactive compound and is removed more rapidly (see equation (2)). The plume observed on 20 July (toluene > benzene) was less processed than the plume observed on 21 July (toluene≈benzene). Scatterplots of benzene and toluene versus CO (Figure 7) show that the ratio of benzene to CO was similar on the 2 d, whereas the ratio of toluene to CO was much lower on 21 July relative to 20 July. Photochemical ages calculated using equation (2) for the plumes on 20 and 21 July are consistent with the transport times estimated from the back trajectories (Figure 6a). The ΔWSOC/ΔCO ratios calculated according to equation (7) agree within 30% with the observations (Table 2).

[43] Also shown in Figure 6d are the measurements of several biogenic VOCs measured by PTR-MS. Isoprene was relatively enhanced, with mixing ratios from 0.5 to 1.0 ppbv over Long Island, but was largely removed on 21 July because of its high reactivity. PTR-MS was also used to quantify the sum of monoterpenes and of the sum of methyl vinyl ketone and methacrolein (MVK + MACR). Relatively low mixing ratios of monoterpenes were observed on both 20 and 21 July; higher mixing ratios were generally found further north in Maine and Nova Scotia in agreement with emission inventories [*Geron et al.*, 2000]. MVK + MACR were the highest on 20 July, but had not been removed entirely on 21 July. These compounds are formed from the oxidation of isoprene and have somewhat longer lifetimes, which explains why they are still observed on 21 July. From the data we conclude that biogenic VOCs were present in the plume from NYC and that they had largely been processed by the time the plume was observed on 21 July.

[44] The analysis in section 3.3 focused entirely on urban VOCs and ignored the fact that biogenic VOCs in urban plumes could play a role in the secondary formation of OM. The mixing ratios of biogenic VOCs measured in

the urban plume on 20 July correspond to mass loadings of 3.1 μg C m^{-3} of MVK + MACR, 2.0 μg C m^{-3} of isoprene and 0.2 μg C m^{-3} of monoterpenes. At OC formation yields of 3% for isoprene and MVK + MACR [*Kroll et al.*, 2005], and 25% for the monoterpenes [*Hoffmann et al.*, 1997], the biogenics could account for an increase of about 0.2 μg C m^{-3}, which is less than 10% of the observed increase in WSOC between 20 and 21 July (Table 2). Most of the transport between 20 and 21 July took place above the ocean, in a layer that was well isolated from the marine boundary layer by a strong inversion, which rules out that biogenic VOCs were continuously added to this air mass during the transport.

4.3. Growth of WSOC in All Urban Plumes

[45] The variation in WSOC as a function of time since emission can be evaluated more systematically. By averaging the aircraft data over the times that the whole air samples (WAS) were collected, the ΔWSOC/ΔCO ratio can be calculated as a function of photochemical age derived from toluene and benzene. This analysis requires a correction to remove the effects of background concentrations on WSOC, CO, and of benzene, all of which have typical lifetimes > 3 d. Background concentrations of these species were determined by averaging measurements taken in air upwind of and adjacent to major urban areas when sampling in plumes <12 h old from identifiable sources. For the more aged plumes, for which a specific source cannot be clearly identified, we subtracted approximate background values for CO (105 ppbv), WSOC (0.25 μg C m^{-3}) and benzene (19 pptv). The background in CO was determined from the maximum in the probability distribution of CO over the continent; backgrounds in WSOC and benzene were determined from scatterplots of those species versus CO, i.e., the WSOC and benzene value at CO of 105 ppbv. Other choices of background correction can be made and were tried over the course of this study; qualitatively the results remained the same.

[46] Figure 8 shows the ΔWSOC/ΔCO ratios in all of the urban plumes observed during ICARTT as a function of the transport age (Figure 8a) and the photochemical age

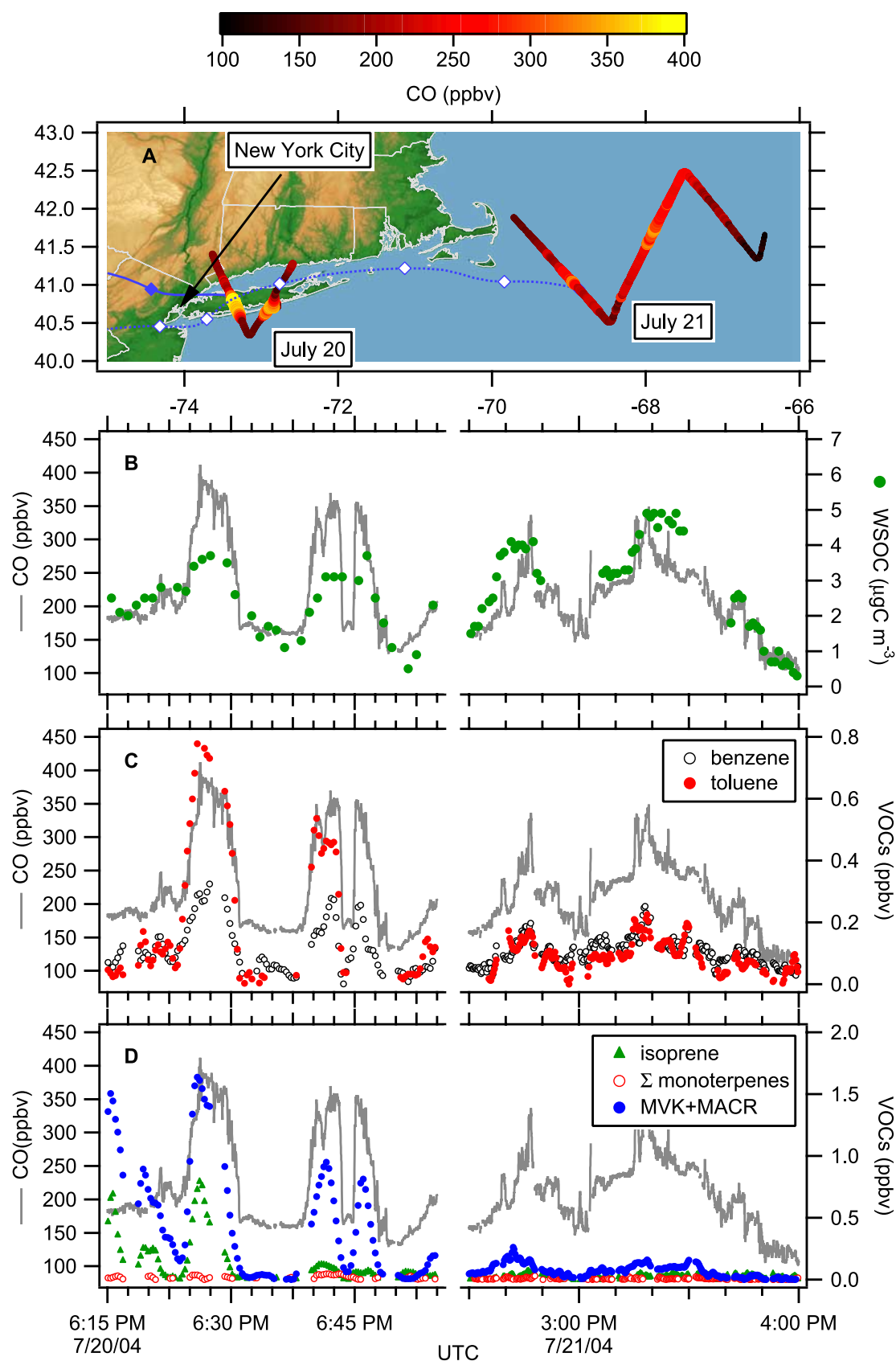**Figure 6.** Results from airborne measurements on 20 and 21 July. (a) Part of the flight tracks color-coded by the measured CO mixing ratio. The blue curves show back trajectories from the highest measured CO, and the solid (20 July) and open (21 July) diamonds show 6-h intervals. Measured (b) CO and WSOC, (c) benzene and toluene and (d) biogenic VOCs obtained for the flight intervals in Figure 6a.
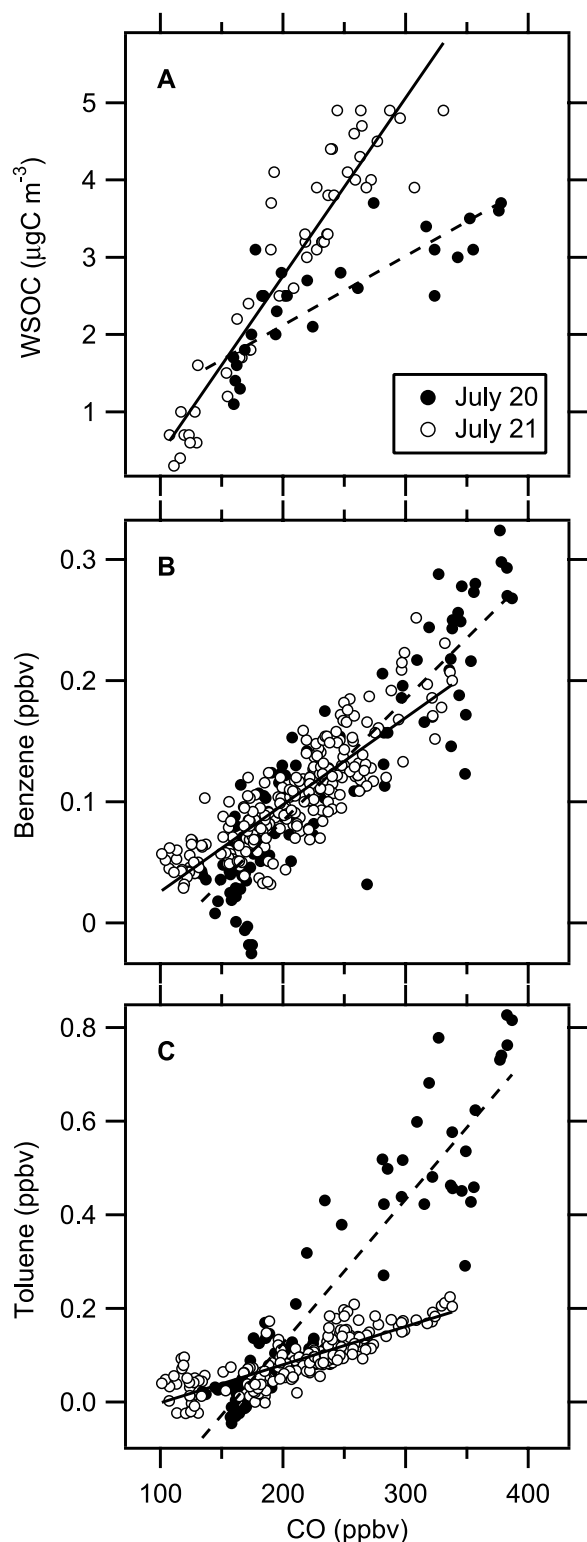
Figure 7. Scatterplots of (a) WSOC, (b) benzene and (c) toluene versus CO for the data shown in Figure 6. Solid circles indicate data from 20 July, and open circles indicate data from 21 July. The dashed (20 July) and solid (21 July) lines show results of linear fits to the data and the results for the slopes and linear correlation coefficients are given in Table 2.

(Figure 8b). Photochemical ages were calculated using equation (2) and the measured enhancements of benzene and toluene. Close to emissions sources, the age could be negative when the measured ratio between toluene and benzene was higher than the estimated emission ratio of 3.7. Transport ages were calculated (1) using measured aircraft winds and surface-based wind profiler data for plumes from identifiable individual sources <6 h old, (2) using trajectories from wind profiler observations for plumes between 6 and 12 h old, and (3) using the Lagrangian transport model FLEXPART [*Stohl et al.*, 2003] for older plumes. Both plots in Figure 8 show that the ΔWSOC/ΔCO ratios in the first hours after emission were significantly lower than after 24 h, indicating the importance of secondary formation in the first day of photochemical processing. The data are overlaid with the ΔWSOC/ΔCO ratio calculated from equation (7), which describes the average increase in the measured ratios reasonably well both in terms of magnitude and timescale (solid blue curve). The data seem to be somewhat lower on average than equation (7), but the difference is well within the limited accuracies of all the data sets involved: equation (7) was based on AMS data from 2002 and converted to WSOC using AMS and WSOC data from 2004 (Figure 1e). Again, it should be noted that the blue curves in Figure 8 do not represent fits of equation (7) to the data fro ICARTT: Figure 8 compares data from ICARTT in 2004 with a semiempirical relationship derived from data from an earlier study in the northeastern United States in 2002 [*de Gouw et al.*, 2005]. The agreement suggests (1) that the observations were consistent between the 2 years and (2) that much of the observed variability in WSOC during ICARTT can be explained by secondary formation in urban plumes.

[47] The ΔWSOC/ΔCO ratios measured from the aircraft at the shortest transport and photochemical ages are low, but not zero according to the literature [*Huang and Yu*, 2007; *Huang et al.*, 2006; *Weber et al.*, 2007]. This is most likely due to the fact that it is difficult to sample air from a dispersed urban source that has not undergone some photochemical processing. Also indicated in Figure 8 are the ΔOC/ΔCO ratios corresponding to primary emissions (5.3 μg C m^{-3} ppmv^{-1}; solid black line), and to the sum of primary emissions and the secondary formation calculated using the yields from *Ng et al.* [2007b] (dotted black line). The ΔWSOC/ΔCO at zero age is similar to the ΔOC/ΔCO for primary, urban emissions; recall that, close to urban sources, the ratio between WSOC and OC changes very rapidly (Figure 2c). After approximately 1 d of photochemical processing, the ΔWSOC/ΔCO ratio far exceeds the primary ΔOC/ΔCO ratio, indicating that the WSOC cannot be primary OC that has oxidized in the particulate phase. The growth in WSOC calculated using the yields from *Ng et al.* [2007b] is at the low end of the range in ΔWSOC/ΔCO ratios observed after 1 d of processing. It is not clear, however, if the primary and secondary contributions can simply be added in this comparison, since primary emissions of WSOC are thought to be zero [*Huang and Yu*, 2007; *Huang et al.*, 2006; *Weber et al.*, 2007]. After 1 d of processing the average ΔWSOC/ΔCO ratio is 23 ± 8 μg C m^{-3} ppmv^{-1} (Figure 8), similar to the analysis by *Sullivan et al.* [2006], whereas the growth in OC expected from the known precursors and yields from *Ng et al.* [2007b] is 7.9 μg C m^{-3} ppmv^{-1}

Table 2. Enhancement Ratios Versus CO of WSOC, Toluene, and Benzene in the Two Urban Plumes Described in Figure 5[a]

| | 20 July | | 21 July | | |
	r^2	Ratio Versus CO	r^2	Ratio Versus CO	Units
WSOC	0.64	8.9 ± 1.2	0.87	23.1 ± 1.2	μg C m^{-3} ppmv^{-1}
Toluene	0.87	3.07 ± 0.12	0.67	0.81 ± 0.04	pptv ppbv^{-1}
Benzene	0.81	1.00 ± 0.05	0.73	0.72 ± 0.03	pptv ppbv^{-1}
	20 July		21 July		Units
Photochemical age	4		25		hours
Calculated ΔWSOC/ΔCO	6.6		26.4		μg C m^{-3} ppmv^{-1}

[a]The last lines contain the photochemical age and WSOC calculated according to equations (3) and (5), respectively.

(ΔOM/ΔCO = 14.1 μg m^{-3} ppmv^{-1}; OM/OC = 1.78 μg μg C^{-1}). This calculated growth in OC represents therefore $34 \pm 12\%$ of the measured increase in WSOC.

4.4. Is CO a Good Tracer for Urban Emissions?

[48] Carbon monoxide (CO) is used in this study as a relatively inert indicator species of urban emissions. On a global scale, however, a significant fraction of CO is not directly emitted but formed from photo-oxidation of methane and VOCs [*Granier et al.*, 2000]. For a number of reasons we argue here that most of the variability in CO observed during ICARTT was driven by direct, urban emissions, and that neglecting the secondary contribution of CO leads to errors in the derived ΔOM/ΔCO ratios of 10 to 20% at most.

[49] The largest secondary source of CO in the atmosphere comes from methane. However, the lifetime of methane is long and this source contributes to the background of CO rather than to the variability observed in the northeastern United States. Formation of CO from biogenic VOCs is the next largest source of secondary CO, and this process occurs within days after emission of the VOCs. Modeling studies indicate that secondary CO from biogenic VOCs contributes less than 20 ppbv CO in the northeastern United States [*Granier et al.*, 2000], which is a small amount compared to the enhancements in CO of 100–200 ppbv that were observed in the urban plumes (Figures 4, 6, and 7). As a result, the error made in the ΔOM/ΔCO ratios in urban plumes is 10–20% at most. *Griffin et al.* [2007] reached a similar conclusion from a modeling study of secondary CO sources in the northeastern United States: these authors concluded that secondary CO contributed at most 10% to the CO measured during ICARTT [*Griffin et al.*, 2007].

[50] In an earlier publication we compared the CO measured during ICARTT with CO calculated from a linear combination of an urban contribution (parameterized by chloroform), a forest fire contribution (parameterized by acetonitrile) and a background of 75 ppbv. The degree of correlation between measured and calculated CO was high with $r^2 = 0.85$, demonstrating that most of the variability in CO could be explained from direct urban and forest fire emissions. To further illustrate this point, we look here at scatterplots of CO versus acetylene (C_2H_2) observed during ICARTT (Figure 9). Acetylene is an urban VOC that we used to parameterize urban emissions in our earlier study [*de Gouw et al.*, 2005]. As acetylene is also emitted from forest fires, the data in Figure 9 were filtered using the measurements of acetonitrile. It is seen that the CO data were correlated with acetylene both in the aircraft ($r^2 = 0.88$) and ship data ($r^2 = 0.75$). Moreover, the data from ICARTT are

overlaid in Figure 9 with data obtained during a research flight of the NOAA WP-3D over Los Angeles in 2002 [*de Gouw et al.*, 2003]. It is seen that the data from ICARTT track the data from Los Angeles very well. In the latter case, secondary CO from biogenic VOCs can be assumed to be negligible [*Griffin et al.*, 2007]. We conclude from Figure 9 that most of the variability in CO is driven by direct, urban emissions of CO, and that secondary CO from biogenic VOCs does not significantly influence the enhancement ratios of trace gases and aerosol species versus CO.

5. Discussion
5.1. Results Consistent With NEAQS 2002

[51] The analyses presented here show that a significant part of the variability observed for OM and WSOC during ICARTT could be explained by the semiempirical equations (5)–(7) derived from our previous work [*de Gouw et al.*, 2005]. Therefore, the current results confirm our previous conclusion that OM (and WSOC) is in large part due to secondary formation in urban plumes. As in our previous work [*de Gouw et al.*, 2005], the secondary formation of OM from biogenic precursors remained difficult to quantify from the measured mass loadings of OM despite the fact that (1) air masses with high monoterpene emissions and evidence for photochemical processing were sampled from both the aircraft and the ship [*Quinn et al.*, 2006; *Weber et al.*, 2007] and (2) the mass spectra obtained by AMS showed signatures of biogenic influences in some of those air masses [*Marcoli et al.*, 2006]. It should be recognized, however, that the secondary OM from biogenic VOCs is typically <3 μg m^{-3} [*Henze and Seinfeld*, 2006; *Tunved et al.*, 2006], which is fairly small in comparison with the mass loadings of 5–15 μg m^{-3} observed in the urban outflow (Figure 5). In other words, the biogenic source of OM could easily be overwhelmed by anthropogenic sources on regional scales.

5.2. What Explains the Strong Growth of OM in Urban Plumes?

[52] In our previous study [*de Gouw et al.*, 2005], there was a large discrepancy between the measured OM growth in urban plumes and the increase calculated from the measured precursors using the particulate yields from *Seinfeld and Pandis* [1998]. We speculated on possible explanations for this discrepancy: (1) OM formation mechanisms are more efficient than chamber studies have indicated, (2) OM is produced from VOCs that are not measured by GC-MS, and (3) the formation of OM from biogenic VOCs is more efficient in urban plumes. Recent studies have addressed in particular the first two possibil-
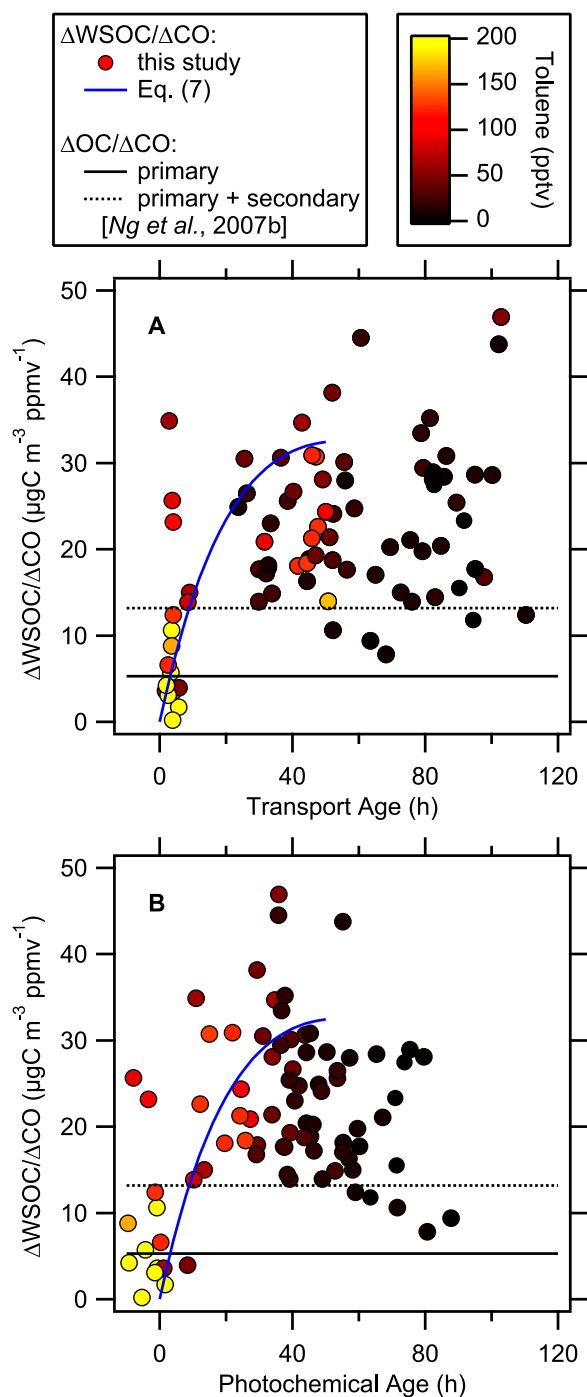
Figure 8. Increase of ∆WSOC/∆CO ratios in urban plumes as a function of (a) transport and (b) photochemical age. The circles show the results from the measurements on board the WP-3D aircraft; the blue, solid curve shows the ∆WSOC/∆CO ratio calculated according to equation (7).

(Figure 8). Both results are significantly higher than the ~7% found in our previous study [*de Gouw et al.*, 2005]. Second, it has been suggested that emissions of semivolatile organic compounds, not measured by GC-MS, provide a large mass fraction of gas-phase emissions from vehicles and are important precursors of secondary formation of OM [*Robinson et al.*, 2007]. We will discuss the formation of OM in urban plumes in light of these new findings in the remainder of this section.

[53] The work of *Seinfeld and Pandis* [1998] is used here as a starting point for the discussion, because it contains a synopsis of prior laboratory work and conveniently lists particulate yields for almost all VOCs measured. However,
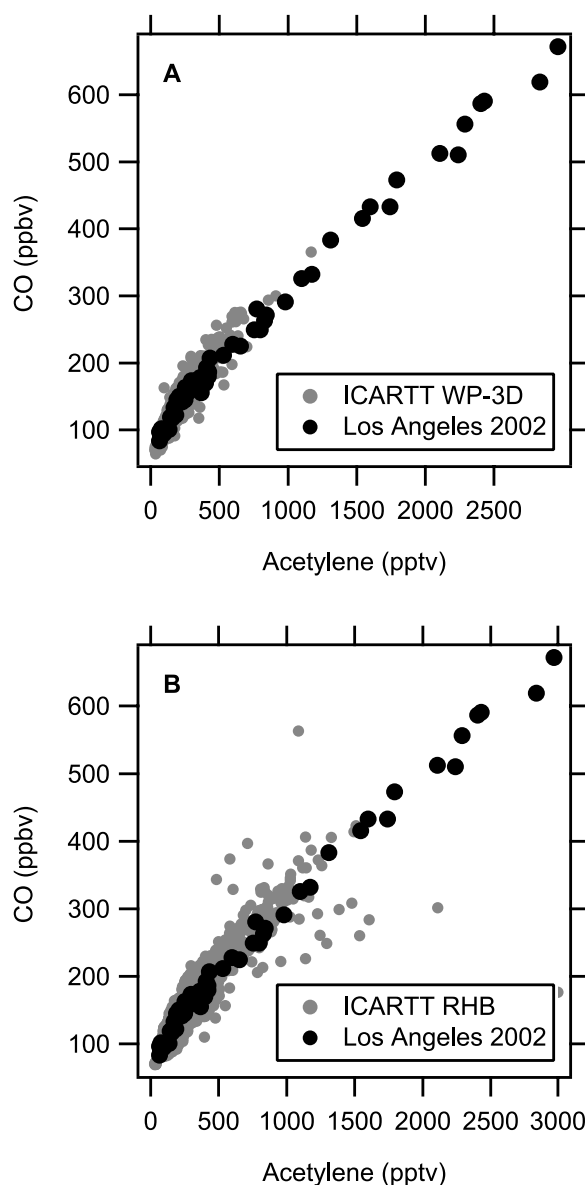
Figure 9. Scatterplots of CO versus acetylene measured on board (a) the WP-3D aircraft and (b) the research ship *Ronald H. Brown*. The data from ICARTT (in gray) are overlaid with data from a flight over Los Angeles in 2002 (in black). Only data with acetonitrile below 200 pptv were used to eliminate air masses influenced by forest fire emissions.

ities. First, new smog chamber results show much higher particulate yields from some aromatic VOCs under conditions of low NOx [*Ng et al.*, 2007b]. We have shown in this study that these newly published yields, extrapolated to all aromatic compounds, explain on average ~37% of the growth in OM observed on board the ship (Figure 4b) and ~34% of the growth in WSOC measured from the aircraft

numerous recent studies indicate that secondary particle formation from some of these VOCs may be more efficient. Particle growth has been observed in chambers from species like isoprene [*Kroll et al.*, 2005] and benzene [*Martin-Reviejo and Wirtz*, 2005; *Ng et al.*, 2007b], which both had zero yields in earlier studies. Particulate mass yields have been found to depend on NOx mixing ratios [*Ng et al.*, 2007b; *Song et al.*, 2005] and may be enhanced by cloud processing [*Ervens et al.*, 2004; *Lim et al.*, 2005]. Acid-catalyzed formation of OM has been observed in chamber studies [*Jang et al.*, 2002], but was not observed during the Pittsburgh Air Quality Study [*Takahama et al.*, 2006] nor in power plant plumes over Atlanta during ICARTT [*Peltier et al.*, 2007b]. Finally, laboratory studies have reported the formation of oligomers, which may lead to higher partitioning of organic material from the gas to the particulate phase [*Kalberer et al.*, 2004].

[54] There is good evidence in the literature that the GC-MS method used in our work to measure VOCs does not allow quantification of all gas-phase carbon. The presence of numerous compounds in urban air that cannot be resolved with conventional chromatography was demonstrated using two-dimensional GC [*Lewis et al.*, 2000]. A fraction of 5–15% of gas-phase organic carbon in unprocessed, urban air was not identified by comparing total to speciated gas-phase organic carbon measurements [*Chung et al.*, 2003]. Indirect evidence is obtained from measurements of the reactivity of OH in urban air, which have shown that in some (but not all) cases the observed reactivity cannot be explained in terms of the measured VOCs [*Ren et al.*, 2006; *Sadanaga et al.*, 2004]. A recent study by *Robinson et al.* [2007] showed that the mass loading of semivolatile organic compounds in vehicle exhaust, which presumably are not measured by GC-MS, could be up to $5\times$ higher than the mass loading of primary OC particles, depending on the degree of dilution of those particles in ambient air. Tunnel studies have shown primary OM versus CO emission ratios of 3.4 μg m^{-3} ppmv^{-1} (section 3.2); emissions of semivolatiles could therefore be as high as 17 μg m^{-3} ppmv^{-1}, which could explain a significant fraction of the growth in OM seen in an urban air mass over the course of 1 d (38 $\pm$ 7 μg m^{-3} ppmv^{-1}; section 4.1) assuming a 100% particulate yield. Nevertheless, there is still much uncertainty regarding the mass fraction and identity of gas-phase organic carbon that is not measured by GC-MS; detailed studies are necessary to assess its potential to form secondary OM.

[55] Laboratory studies have shown that biogenic VOCs can be very efficient precursors for OM formation [*Hoffmann et al.*, 1997; *Kroll et al.*, 2005], and their emissions are significant in the forested northeastern United States. The robust correlations of OM and WSOC with the anthropogenic tracer gas CO argue against a strong biogenic source relative to the urban source. Also, we showed above that the concentrations of biogenic VOCs in the New York City plume were not high enough to explain the observed growth of OM using published particulate yields. The same argument used above for anthropogenic VOCs may also hold for the biogenic VOCs; that is, there may biogenic species of lower volatility not measured by current techniques that may be important OM precursors [*Goldstein and Galbally*, 2007]. This would not explain, however, why OM and CO are correlated so well on regional scales. If the

formation of OM from biogenic precursors is more efficient in urban plumes, this could explain (1) why OM and CO are correlated and (2) why the modern (biogenic) fraction of OM is very high according to most radiocarbon dating studies [*Klinedinst and Currie*, 1999; *Lemire et al.*, 2002; *Szidat et al.*, 2004]. Evidence for increased formation of secondary OM at elevated levels of NOx, i.e., in pollution plumes, has been reported for two sesquiterpene species [*Ng et al.*, 2007a]. However, the magnitude of the effect (a factor of 2 enhancement at a NOx level of 500 ppbv) may not be enough to explain the observations reported here, in addition to the fact that for other biogenic VOCs the SOA yields are higher at low NOx. Also, no SOA formation was reported in power plant plumes near Atlanta, Georgia, with high NOx, high biogenic VOCs but no anthropogenic VOCs [*Peltier et al.*, 2007b].

[56] Biomass burning is a large source of OM to the global atmosphere, but has not been discussed so far in this paper. The emissions of forest fires were clearly identifiable in the ICARTT data set, and those air masses were explicitly removed for the purpose of this study. There are, however, biomass-burning sources in urban atmospheres such as waste burning, charbroiling and wood stoves. We have assumed that their emissions are part of the regular "urban" mixture of emissions of OM and VOCs instead of treating them explicitly as a separate source. Other studies have shown that biomass burning may be responsible for much of the primary OM emissions in urban air [*Lanz et al.*, 2006; *Schauer et al.*, 1996], and presumably the highly oxygenated VOCs released from burning could be efficient OM precursors as well. Overall, however, we would expect biomass burning to be a relatively minor summertime source of OM in cities in the northeastern United States.

[57] The results presented here and elsewhere strongly suggest that OM is significantly influenced by anthropogenic emissions over relatively large parts of the United States. This conclusion implies that OM concentrations may be decreased by a reduction in anthropogenic VOC emissions. However, the formation of OM is insufficiently understood to develop a target emissions control strategy or to assess the effectiveness of emissions reductions.

5.3. Significance of Secondary OM Formation From Urban VOCs

[58] This work has shown that secondary formation from urban VOCs can be a regionally important, if not dominant, source of OM. How important is this source on global and continental scales? Here, we estimate the global source of secondary formation from urban VOCs using the fossil-fuel-related emissions of CO of 244 Tg a^{-1} in EDGAR 3.2 (Emission Database for Global Atmospheric Research [*Olivier et al.*, 2005]) and the OM yield of 38 $\pm$ 7 μg m^{-3} ppmv^{-1} (section 4.1). The result is a global source of 8.0 Tg a^{-1} (Table 3) with an estimated uncertainty of 50% that includes uncertainties in both the OM yield (20%) and the EDGAR inventory (30%). According to EDGAR 3.2, the United States is responsible for 25.9% of the fossil-fuel-related CO emissions, and therefore the U.S. source of secondary OM from urban VOCs is 2.1 Tg a^{-1} (Table 3). For comparison, Table 3 summarizes several other estimates of global sources of OM and the U.S. contribution. The primary emissions estimates are taken from a fuel-based

Table 3. Estimated Source Budget of Organic Matter (OM) in the Global Atmosphere and the U.S. Contribution[a]

Description	Global Source, Tg a^{-1}	U.S. Contribution %	U.S. Contribution Tg a^{-1}
Primary Sources			
Open biomass burning[b]	**40** (21−91)[c,d]	3.4[c]	**1.3** (0.7−3.1)
Biofuel use	**10.4** (5.0−21)[c,d]	4.3[c]	**0.4** (0.2−0.9)
Fossil fuel use	**3.8** (1.9−11)[c,d]	10.4[c]	**0.4** (0.2−1.2)
Secondary Formation			
Isoprene	**6.2** (2−6.2)[e,f]	4.8[g]	**0.3** (0.1−0.3)
Terpenes	**10.2** (10.2−19.1)[e,h]	6.3[g]	**0.6** (0.6−1.2)
Other biogenic VOCs	**15** (5−25)[h]	5.0[g]	**0.8** (0.3−1.3)
Urban VOCs	**8.0** (4.0−12)	25.9[i]	**2.1** (1.0−3.1)
Total	**94** (49−185)		**6.0** (4.7−17)

[a]Best estimates are bold; uncertainty ranges in parentheses.
[b]Includes savanna and forest fires, and agricultural burning.
[c]*Bond et al.* [2004].
[d]*Henze and Seinfeld* [2006].
[e]*Henze and Seinfeld* [2006].
[f]*Claeys et al.* [2004].
[g]*Guenther et al.* [1995].
[h]*Kanakidou et al.* [2005].
[i]EDGAR 3.2 [*Olivier et al.*, 2005].

inventory [*Bond et al.*, 2004], whereas estimates of the secondary formation from biogenic VOCs are from two papers [*Claeys et al.*, 2004; *Henze and Seinfeld*, 2006] and a recent review [*Kanakidou et al.*, 2005].

[59] Globally, the dominant primary source of OM is from open biomass burning: savanna and forest fires, and to a lesser extent agricultural burning [*Bond et al.*, 2004]. Most of this burning takes place in Africa and South America, and the U.S. contribution is only 3.4%. Sources of primary OM related to the use of biofuel and fossil fuels are smaller on a global scale. The estimate for the U.S. source of OM from fossil fuel use is 0.4 Tg a^{-1} (Table 3). We can compare this to an estimate derived from the emission ratio of OM relative to CO (9.4 μg m^{-3} ppmv^{-1}; section 3.1) and the U.S. emissions of CO from fossil fuel use (63.2 Tg a^{-1} EDGAR 3.2), and arrive at 0.5 Tg a^{-1}. The good agreement with the estimate from *Bond et al.* [2004] lends further credence to our primary emissions estimates.

[60] We consider the secondary formation from isoprene, terpenes and other reactive biogenic VOCs separately in Table 3. Global estimates of secondary OM from isoprene range from 2 Tg a^{-1} [*Claeys et al.*, 2004] to 6.2 Tg a^{-1} [*Henze and Seinfeld*, 2006]. We take the second number, derived from a global model, as our best estimate in Table 3. Estimates for secondary OM formation from monoterpenes range from 10.2 Tg a^{-1} [*Henze and Seinfeld*, 2006] to 19.1 Tg a^{-1} [*Kanakidou et al.*, 2005]. In this case, we take the lower number as our best estimate: the result from *Kanakidou et al.* [2005] was obtained using a particulate yield of 15%, whereas recent field observations have suggested a lower yield of 7.5% [*Tunved et al.*, 2006]. Much more uncertain is the secondary source of OM from other reactive biogenic VOCs (sesquiterpenes etc.). An estimate is included in Table 3, but the uncertainty ranges over a factor of 5 [*Kanakidou et al.*, 2005]. Most biogenic emissions take place in the tropics due a longer growing season and higher temperatures; the U.S. contribution of isoprene and terpene emissions are only 4.8% and 6.3%, respectively, of the global emissions [*Guenther et al.*, 1995]. As a result, the U.S. sources of OM from these biogenic

VOCs are relatively small at 5% and 10% of the global OM source.

[61] In comparison with the primary emission sources and the secondary formation from biogenic VOCs, the secondary OM formation from urban VOCs is a relatively minor, though not insignificant global source at ~8.5%. However, at northern temperate latitudes this percentage is much higher since a large fraction of fossil fuel consumption takes place in the United States, western Europe and east Asia, whereas biogenic emissions and biomass burning are mostly located in the tropics. As a result, secondary OM from urban VOCs contributes significantly more at ~35% of the total source in the United States (Table 3). All of these source estimates clearly have large uncertainties, and much more work is needed to corroborate these results. In addition, there is a strong seasonality in the source estimates for North America, with higher forest fire and biogenic emissions as well as a more active photochemistry in the summer. It would be of interest to study the formation of secondary OM in urban plumes in the wintertime: do lower radical levels merely slow the formation down, or result in different particulate yields? What is the effect of different VOC emissions in the wintertime, and do lower temperatures affect secondary OM significantly because of the effects on vapor pressure?

6. Conclusion

[62] These new observations and a growing body of evidence in the recent literature show that the secondary formation of OM from anthropogenic VOCs emitted from urban sources can be an important source on regional scales. Similar, earlier work suggested that the production of secondary OM in urban air could not be explained using the measured emissions of known precursors and their particulate yields determined from smog chamber studies. However, newly published particulate yields for aromatic VOCs are much higher, reducing the discrepancy from an order of magnitude to a factor of ~3. In addition, the secondary formation from some semivolatile compounds released by motor vehicles and other sources, which compounds are not measured using GC-MS, may help explain the remaining discrepancy. If anthropogenic gas-phase compounds are indeed much more efficient precursors of OM than previously recognized, then a reduction in their emissions could mitigate the air quality and climate effects of OM. More research is required, however, to quantify the sources, and the mechanisms and efficiency of secondary OM formation in urban air.

References

Allan, J. D., et al. (2004), Submicron aerosol composition at Trinidad Head, California, during ITCT 2K2: Its relationship with gas phase volatile organic carbon and assessment of instrument performance, *J. Geophys. Res.*, 109, D23S24, doi:10.1029/2003JD004208.

Atkinson, R., and J. Arey (2003), Atmospheric degradation of volatile organic compounds, *Chem. Rev.*, 103, 4605−4638, doi:10.1021/cr0206420.

Bahreini, R., et al. (2003), Aircraft-based aerosol size and composition measurements during ACE-Asia using an Aerodyne aerosol mass spectrometer, *J. Geophys. Res.*, 108(D23), 8645, doi:10.1029/2002JD003226.

Bates, T. S., P. K. Quinn, D. J. Coffman, J. E. Johnson, and A. M. Middlebrook (2005), Dominance of organic aerosols in the marine boundary layer over the Gulf of Maine during NEAQS 2002 and their role in aerosol light scattering, *J. Geophys. Res.*, *110*, D18202, doi:10.1029/2005JD005797.

Bond, T. C., D. G. Streets, K. F. Yarber, S. M. Nelson, J. H. Woo, and Z. Klimont (2004), A technology-based global inventory of black and organic carbon emissions from combustion, *J. Geophys. Res.*, *109*, D14203, doi:10.1029/2003JD003697.

Brock, C. A., et al. (2008), Sources of particulate matter in the northeastern United States in summer: 2. Evolution of chemical and microphysical properties in urban plumes, *J. Geophys. Res.*, doi:10.1029/2007JD009241, in press.

Canagaratna, M. R., et al. (2007), Chemical and microphysical characterization of ambient aerosols with the aerodyne aerosol mass spectrometer, *Mass Spectrom. Rev.*, *26*, 185–222, doi:10.1002/mas.20115.

Chung, M. Y., C. Maris, U. Krischke, R. Meller, and S. E. Paulson (2003), An investigation of the relationship between total non-methane organic carbon and the sum of speciated hydrocarbons and carbonyls measured by standard GC/FID: Measurements in the Los Angeles air basin, *Atmos. Environ.*, *37*, S159–S170, doi:10.1016/S1352-2310(03)00388-1.

Claeys, M., et al. (2004), Formation of secondary organic aerosols through photooxidation of isoprene, *Science*, *303*, 1173–1176, doi:10.1126/science.1092805.

de Gouw, J. A., and C. Warneke (2007), Measurements of volatile organic compounds in the Earth's atmosphere using proton-transfer-reaction mass spectrometry, *Mass Spectrom. Rev.*, *26*, 223–257, doi:10.1002/mas.20119.

de Gouw, J. A., C. Warneke, D. D. Parrish, J. S. Holloway, M. Trainer, and F. C. Fehsenfeld (2003), Emission sources and ocean uptake of acetonitrile (CH_3CN) in the atmosphere, *J. Geophys. Res.*, *108*(D11), 4329, doi:10.1029/2002JD002897.

de Gouw, J. A., et al. (2005), Budget of organic carbon in a polluted atmosphere: Results from the New England Air Quality Study in 2002, *J. Geophys. Res.*, *110*, D16305, doi:10.1029/2004JD005623.

de Gouw, J. A., et al. (2006), Volatile organic compounds composition of merged and aged forest fire plumes from Alaska and western Canada, *J. Geophys. Res.*, *111*, D10303, doi:10.1029/2005JD006175.

Donahue, N. M., A. L. Robinson, C. O. Stanier, and S. N. Pandis (2006), Coupled partitioning, dilution, and chemical aging of semivolatile organics, *Environ. Sci. Technol.*, *40*, 2635–2643, doi:10.1021/es052297c.

Ervens, B., G. Feingold, G. J. Frost, and S. M. Kreidenweis (2004), A modeling study of aqueous production of dicarboxylic acids: 1. Chemical pathways and speciated organic mass production, *J. Geophys. Res.*, *109*, D15205, doi:10.1029/2003JD004387.

Fehsenfeld, F. C., et al. (2006), International Consortium for Atmospheric Research on Transport and Transformation (ICARTT): North America to Europe-Overview of the 2004 summer field study, *J. Geophys. Res.*, *111*, D23S01, doi:10.1029/2006JD007829.

Gerbig, C., S. Smitgen, D. Kley, A. Volz-Thomas, H. Dewey, and D. Haaks (1999), An improved fast response vacuum UV resonance fluorescence CO instrument, *J. Geophys. Res.*, *104*, 1699–1704.

Geron, C., R. Rasmussen, R. R. Arnts, and A. Guenther (2000), A review and synthesis of monoterpene speciation from forests in the United States, *Atmos. Environ.*, *34*, 1761–1781, doi:10.1016/S1352-2310(99)00364-7.

Goldan, P. D., W. C. Kuster, E. Williams, P. C. Murphy, F. C. Fehsenfeld, and J. Meagher (2004), Nonmethane hydrocarbon and oxy hydrocarbon measurements during the 2002 New England Air Quality Study, *J. Geophys. Res.*, *109*, D21309, doi:10.1029/2003JD004455.

Goldstein, A. H., and I. E. Galbally (2007), Known and unexplored organic constituents in the Earth's atmosphere, *Environ. Sci. Technol.*, *41*, 1514–1521.

Granier, C., G. Petron, J.-F. Muller, and G. Brasseur (2000), The impact of natural and anthropogenic hydrocarbons on the tropospheric budget of carbon monoxide, *Atmos. Environ.*, *34*, 5255–5270, doi:10.1016/S1352-2310(00)00299-5.

Griffin, R. J., D. Dabdub, and J. H. Seinfeld (2005), Development and initial evaluation of a dynamic species-resolved model for gas phase chemistry and size-resolved gas/particle partitioning associated with secondary organic aerosol formation, *J. Geophys. Res.*, *110*, D05304, doi:10.1029/2004JD005219.

Griffin, R. J., J. Chen, K. Carmody, S. Vutukuru, and D. Dabdub (2007), Contribution of gas phase oxidation of volatile organic compounds to atmospheric carbon monoxide levels in two areas of the United States, *J. Geophys. Res.*, *112*, D10S17, doi:10.1029/2006JD007602.

Guenther, A., et al. (1995), A global model of natural volatile organic compound emissions, *J. Geophys. Res.*, *100*, 8873–8892.

Heald, C. L., et al. (2005), A large organic aerosol source in the free troposphere missing from current models, *Geophys. Res. Lett.*, *32*, L18809, doi:10.1029/2005GL023831.

Henze, D. K., and J. H. Seinfeld (2006), Global secondary organic aerosol from isoprene oxidation, *Geophys. Res. Lett.*, *33*, L09812, doi:10.1029/2006GL025976.

Hoffmann, T., et al. (1997), Formation of organic aerosols from the oxidation of biogenic hydrocarbons, *J. Atmos. Chem.*, *26*, 189–222, doi:10.1023/A:1005734301837.

Holloway, J. S., et al. (2000), Airborne intercomparison of vacuum ultraviolet fluorescence and tunable diode laser absorption measurements of tropospheric carbon monoxide, *J. Geophys. Res.*, *105*, 24,251–24,261.

Huang, X. F., and J. Z. Yu (2007), Is vehicle exhaust a significant primary source of oxalic acid in ambient aerosols?, *Geophys. Res. Lett.*, *34*, L02808, doi:10.1029/2006GL028457.

Huang, X. F., J. Z. Yu, L. Y. He, and Z. Yuan (2006), Water-soluble organic carbon and oxalate in aerosols at a coastal urban site in China: Size distribution characteristics, sources, and formation mechanisms, *J. Geophys. Res.*, *111*, D22212, doi:10.1029/2006JD007408.

Jang, M. S., N. M. Czoschke, S. Lee, and R. M. Kamens (2002), Heterogeneous atmospheric aerosol production by acid-catalyzed particle-phase reactions, *Science*, *298*, 814–817, doi:10.1126/science.1075798.

Jayne, J. T., D. C. Leard, X. Zhang, P. Davidovits, K. A. Smith, C. E. Kolb, and D. R. Worsnop (2000), Development of an aerosol mass spectrometer for size and composition analysis of submicron particles, *Aerosol Sci. Technol.*, *33*, 49–70, doi:10.1080/027868200410840.

Johnson, D., et al. (2006), Simulating regional scale secondary organic aerosol formation during the TORCH 2003 campaign in the southern UK, *Atmos. Chem. Phys.*, *6*, 403–418.

Kalberer, M., et al. (2004), Identification of polymers as major components of atmospheric organic aerosols, *Science*, *303*, 1659–1662, doi:10.1126/science.1092185.

Kanakidou, M., et al. (2005), Organic aerosol and global climate modelling: A review, *Atmos. Chem. Phys.*, *5*, 1053–1123.

Kirchstetter, T. W., R. A. Harley, N. M. Kreisberg, M. R. Stolzenburg, and S. V. Hering (1999), On-road measurement of fine particle and nitrogen oxide emissions from light- and heavy-duty motor vehicles, *Atmos. Environ.*, *33*, 2955–2968, doi:10.1016/S1352-2310(99)00089-8.

Klinedinst, D. B., and L. A. Currie (1999), Direct quantification of PM2.5 fossil and biomass carbon within the Northern Front Range Air Quality Study's domain, *Environ. Sci. Technol.*, *33*, 4146–4154, doi:10.1021/es990355m.

Kondo, Y., et al. (2007), Oxygenated and water-soluble organic aerosols in Tokyo, *J. Geophys. Res.*, *112*, D01203, doi:10.1029/2006JD007056.

Kroll, J. H., N. L. Ng, S. M. Murphy, R. C. Flagan, and J. H. Seinfeld (2005), Secondary organic aerosol formation from isoprene photooxidation under high-NOx conditions, *Geophys. Res. Lett.*, *32*, L18808, doi:10.1029/2005GL023637.

Kroll, J. H., N. L. Ng, S. M. Murphy, R. C. Flagan, and J. H. Seinfeld (2006), Secondary organic aerosol formation from isoprene photooxidation, *Environ. Sci. Technol.*, *40*, 1869–1877, doi:10.1021/es0524301.

Lanz, V. A., M. R. Alfarra, U. Baltensperger, B. Buchmann, C. Hueglin, and A. S. H. Prevot (2006), Source apportionment of submicron organic aerosol at an urban site by linear unmixing of aerosol mass spectra, *Atmos. Chem. Phys.*, *7*, 1503–1522.

Lemire, K. R., D. T. Allen, G. A. Klouda, and C. W. Lewis (2002), Fine particulate matter source attribution for southeast Texas using ^{14}C/^{13}C ratios, *J. Geophys. Res.*, *107*(D22), 4613, doi:10.1029/2002JD002339.

Lewis, A. C., et al. (2000), A larger pool of ozone-forming carbon compounds in urban atmospheres, *Nature*, *405*, 778–781, doi:10.1038/35015540.

Lim, H. J., and B. J. Turpin (2002), Origins of primary and secondary organic aerosol in Atlanta: Results' of time-resolved measurements during the Atlanta supersite experiment, *Environ. Sci. Technol.*, *36*, 4489–4496, doi:10.1021/es0206487.

Lim, H. J., A. G. Carlton, and B. J. Turpin (2005), Isoprene forms secondary organic aerosol through cloud processing: Model simulations, *Environ. Sci. Technol.*, *39*, 4441–4446, doi:10.1021/es048039h.

Mader, B. T., et al. (2003), Sampling methods used for the collection of particle-phase organic and elemental carbon during ACE-Asia, *Atmos. Environ.*, *37*, 1435–1449, doi:10.1016/S1352-2310(02)01061-0.

Marcoli, C., et al. (2006), Cluster analysis of the organic peaks in bulk mass spectra obtained during the 2002 New England Air Quality Study with an Aerodyne aerosol mass spectrometer, *Atmos. Chem. Phys.*, *6*, 5649–5666.

Maria, S. F., L. M. Russell, M. K. Gilles, and S. C. B. Myneni (2004), Organic aerosol growth mechanisms and their climate-forcing implications, *Science*, *306*, 1921–1924, doi:10.1126/science.1103491.

Martin-Reviejo, M., and K. Wirtz (2005), Is benzene a precursor for secondary organic aerosol?, *Environ. Sci. Technol.*, *39*, 1045–1054, doi:10.1021/es049802a.

McKeen, S. A., et al. (2007), Evaluation of several PM2.5 forecast models using data collected during the ICARTT/NEAQS 2004 field study, *J. Geophys. Res.*, *112*, D10S20, doi:10.1029/2006JD007608.

Murphy, D. M., et al. (2006), Single-particle mass spectrometry of tropospheric aerosol particles, *J. Geophys. Res.*, *111*, D23S32, doi:10.1029/2006JD007340.

Neuman, J. A., et al. (2006), Reactive nitrogen transport and photochemistry in urban plumes over the North Atlantic Ocean, *J. Geophys. Res.*, *111*, D23S54, doi:10.1029/2005JD007010.

Ng, N. L., et al. (2007a), Effect of NOx level on secondary organic aerosol (SOA) formation from the photooxidation of terpenes, *Atmos. Chem. Phys. Disc.*, *7*, 10,131–10,177.

Ng, N. L., J. H. Kroll, A. W. H. Chan, P. S. Chhabra, R. C. Flagan, and J. H. Seinfeld (2007b), Secondary organic aerosol formation from m-xylene, toluene, and benzene, *Atmos. Chem. Phys.*, *7*, 3909–3922.

Odum, J. R., T. P. W. Jungkamp, R. J. Griffin, R. C. Flagan, and J. H. Seinfeld (1997), The atmospheric aerosol-forming potential of whole gasoline vapor, *Science*, *276*, 96–99, doi:10.1126/science.276.5309.96.

Olivier, J. G. J., J. A. van Aardenne, F. Dentener, L. Ganzeveld, and J. A. H. W. Peters (2005), Recent trends in global greenhouse gas emissions: regional trends and spatial distribution of key sources, in *Non-CO2 Greenhouse Gases (NCGG-4)*, edited by A. van Amstel, pp. 325–330, Millpress, Rotterdam, Netherlands.

Parrish, D. D. (2006), Critical evaluation of US on-road vehicle emission inventories, *Atmos. Environ.*, *40*, 2288–2300, doi:10.1016/j.atmosenv.2005.11.033.

Peltier, R. E., et al. (2007a), Fine aerosol bulk composition measured on WP-3D research aircraft in vicinity of the northeastern United States—Results from NEAQS, *Atmos. Chem. Phys.*, *7*, 3231–3247.

Peltier, R. E., et al. (2007b), No evidence for acid-catalyzed secondary organic aerosol formation in power-plant plumes over metropolitan Atlanta,Georgia, *Geophys. Res. Lett.*, *34*, L06801, doi:10.1029/2006GL028780.

Pfister, G., et al. (2005), Quantifying CO emissions from the 2004 Alaskan wildfires using MOPITT CO data, *Geophys. Res. Lett.*, *32*, L11809, doi:10.1029/2005GL022995.

Quinn, P. K., and T. S. Bates (2003), North American, Asian, and Indian haze: Similar regional impacts on climate?, *Geophys. Res. Lett.*, *30*(11), 1555, doi:10.1029/2003GL016934.

Quinn, P. K., et al. (2006), Impacts of sources and aging on submicrometer aerosol properties in the marine boundary layer across the Gulf of Maine, *J. Geophys. Res.*, *111*, D23S36, doi:10.1029/2006JD007582.

Ramanathan, V., P. J. Crutzen, J. T. Kiehl, and D. Rosenfeld (2001), Atmosphere—Aerosols, climate, and the hydrological cycle, *Science*, *294*, 2119–2124, doi:10.1126/science.1064034.

Ren, X. R., et al. (2006), OH, HO2, and OH reactivity during the PMTACS-NY Whiteface Mountain 2002 campaign: Observations and model comparison, *J. Geophys. Res.*, *111*, D10S03, doi:10.1029/2005JD006126.

Robinson, A. L., et al. (2007), Rethinking organic aerosols: Semivolatile emissions and photochemical aging, *Science*, *315*, 1259–1262, doi:10.1126/science.1133061.

Sadanaga, Y., et al. (2004), The importance of NO2 and volatile organic compounds in the urban air from the viewpoint of the OH reactivity, *Geophys. Res. Lett.*, *31*, L08102, doi:10.1029/2004GL019661.

Schauer, J. J., and G. R. Cass (2000), Source apportionment of wintertime gas-phase and particle-phase air pollutants using organic compounds as tracers, *Environ. Sci. Technol.*, *34*, 1821–1832, doi:10.1021/es981312t.

Schauer, J. J., W. F. Rogge, L. M. Hildemann, M. A. Mazurek, and G. R. Cass (1996), Source apportionment of airborne particulate matter using organic compounds as tracers, *Atmos. Environ.*, *30*, 3837–3855, doi:10.1016/1352-2310(96)00085-4.

Schauer, J. J., et al. (2003), ACE-Asia intercomparison of a thermal-optical method for the determination of particle-phase organic and elemental carbon, *Environ. Sci. Technol.*, *37*, 993–1001, doi:10.1021/es020622.

Schauffler, S., et al. (1999), Distributions of brominated organic compounds in the troposphere and lower stratosphere, *J. Geophys. Res.*, *104*, 21,513–21,535.

Seinfeld, J. H., and S. N. Pandis (1998), *Atmospheric Chemistry and Physics,* pp. 700–765, John Wiley, New York.

Song, C., K. S. Na, and D. R. Cocker (2005), Impact of the hydrocarbon to NOx ratio on secondary organic aerosol formation, *Environ. Sci. Technol.*, *39*, 3143–3149, doi:10.1021/es0493244.

Stohl, A., et al. (2003), A backward modeling study of intercontinental pollution transport using aircraft measurements, *J. Geophys. Res.*, *108*(D12), 4370, doi:10.1029/2002JD002862.

Sullivan, A. P., R. J. Weber, A. L. Clements, J. R. Turner, M. S. Bae, and J. J. Schauer (2004), A method for on-line measurement of water-soluble organic carbon in ambient aerosol particles: Results from an urban site, *Geophys. Res. Lett.*, *31*, L13105, doi:10.1029/2004GL019681.

Sullivan, A. P., et al. (2006), Airborne measurements of carbonaceous aerosol soluble in water over northeastern United States: Method development and an investigation into water-soluble organic carbon sources, *J. Geophys. Res.*, *111*, D23S46, doi:10.1029/2006JD007072.

Szidat, S., et al. (2004), Radiocarbon (C-14)-deduced biogenic and anthropogenic contributions to organic carbon (OC) of urban aerosols from Zurich, Switzerland, *Atmos. Environ.*, *38*, 4035–4044, doi:10.1016/j.atmosenv.2004.03.066.

Takahama, S., C. I. Davidson, and S. N. Pandis (2006), Semicontinuous measurements of organic carbon and acidity during the Pittsburgh air quality study: Implications for acid-catalyzed organic aerosol formation, *Environ. Sci. Technol.*, *40*, 2191–2199.

Takegawa, N., et al. (2006a), Evolution of submicron organic aerosol in polluted air exported from Tokyo, *Geophys. Res. Lett.*, *33*, L15814, doi:10.1029/2006GL025815.

Takegawa, N., et al. (2006b), Seasonal and diurnal variations of submicron organic aerosol in Tokyo observed using the Aerodyne aerosol mass spectrometer, *J. Geophys. Res.*, *111*, D11206, doi:10.1029/2005JD006515.

Tsigaridis, K., and M. Kanakidou (2007), Secondary organic aerosol importance in the future atmosphere, *Atmos. Environ.*, *41*, 4682–4692, doi:10.1016/j.atmosenv.2007.03.045.

Tunved, P., et al. (2006), High natural aerosol loading over boreal forests, *Science*, *312*, 261–263, doi:10.1126/science.1123052.

Turpin, B. J., and J. J. Huntzicker (1995), Identification of secondary organic aerosol episodes and quantitation of primary and secondary organic aerosol concentrations during SCAQS, *Atmos. Environ.*, *29*, 3527–3544, doi:10.1016/1352-2310(94)00276-Q.

Turpin, B. J., and H. J. Lim (2001), Species contributions to PM2.5 mass concentrations: Revisiting common assumptions for estimating organic mass, *Aerosol Sci. Technol.*, *35*, 602–610, doi:10.1080/02786820152051454.

Volkamer, R., et al. (2006), Secondary organic aerosol formation from anthropogenic air pollution: Rapid and higher than expected, *Geophys. Res. Lett.*, *33*, L17811, doi:10.1029/2006GL026899.

Warneke, C., et al. (2005), Online volatile organic compound measurements using a newly developed proton-transfer ion-trap mass spectrometry instrument during New England Air Quality Study-Intercontinental Transport and Chemical Transformation 2004: Performance, intercomparison, and compound identification, *Environ. Sci. Technol.*, *39*, 5390–5397, doi:10.1021/es050602o.

Warneke, C., et al. (2006), Biomass burning and anthropogenic sources of CO over New England in the summer 2004, *J. Geophys. Res.*, *111*, D23S15, doi:10.1029/2005JD006878.

Warneke, C., et al. (2007), Measurements of urban volatile organic compound emission ratios and comparison with an emissions database, *J. Geophys. Res.*, *112*, D10S47, doi:10.1029/2006JD007930.

Weber, R. J., et al. (2007), A study of secondary organic aerosol formation in the anthropogenic-influenced southeastern United States, *J. Geophys. Res.*, *112*, D13302, doi:10.1029/2007JD008408.

Wert, B., et al. (2003), Signatures of terminal alkene oxidation in airborne formaldehyde measurements during TexAQS 2000, *J. Geophys. Res.*, *108*(D3), 4104, doi:10.1029/2002JD002502.

Zhang, Q., et al. (2005a), Deconvolution and quantification of hydrocarbon-like and oxygenated organic aerosols based on aerosol mass spectrometry, *Environ. Sci. Technol.*, *39*, 4938–4952, doi:10.1021/es048568l.

Zhang, Q., D. R. Worsnop, M. R. Canagaratna, and J. L. Jimenez (2005b), Hydrocarbon-like and oxygenated organic aerosols in Pittsburgh: Insights into sources and processes of organic aerosols, *Atmos. Chem. Phys.*, *5*, 3289–3311.

Zhang, Q., et al. (2007), Ubiquity and dominance of oxygenated species in organic aerosols in anthropogenically-influenced Northern Hemisphere midlatitudes, *Geophys. Res. Lett.*, *34*, L13801, doi:10.1029/2007GL029979.

————————————

E. L. Atlas, Rosenstiel School of Marine and Atmospheric Science, University of Miami, Miami, FL 33149, USA.

T. S. Bates and P. K. Quinn, Pacific Marine Environment Laboratory, NOAA, Seattle, WA 98115, USA.

C. A. Brock, J. A. de Gouw, F. C. Fehsenfeld, P. D. Goldan, J. S. Holloway, W. C. Kuster, B. M. Lerner, A. M. Middlebrook, C. J. Senff, M. Trainer, C. Warneke, and E. J. Williams, Chemical Sciences Division, Earth System Research Laboratory, NOAA, Boulder, CO 80305, USA. (joost.degouw@noaa.gov)

B. M. Matthew, Eastman Kodak Company, 9952 Eastman Park Drive, Windsor, CO 80550, USA.

T. B. Onasch, Aerodyne Research Inc., Billerica, MA 01821, USA.

R. E. Peltier, Department of Environmental Medicine, New York University School of Medicine, Tuxedo, NY 10987, USA.

A. Stohl, Norwegian Institute for Air Research, N-2027 Kjeller, Norway.

A. P. Sullivan, Department of Atmospheric Science, Colorado State University, Fort Collins, CO 80523, USA.

R. J. Weber, School of Earth and Atmospheric Sciences, Georgia Institute of Technology, Atlanta, GA 30332, USA.